Franziska Fichtner | Francois F. Barbier | Maria Grazia Annunziata |
Regina Feil | Justyna Jadwiga Olas | Bernd Müller-Röber | Mark Stitt |
Christine A. Beveridge | John Edward Lunn

Regulation of shoot branching in arabidopsis by trehalose 6-phosphate

Journal article | Version of record

Regulation of shoot branching in arabidopsis by trehalose 6-phosphate

Franziska Fichtner[1,2] (ID), **Francois F. Barbier**[2] (ID), **Maria G. Annunziata**[1] (ID), **Regina Feil**[1] (ID), **Justyna J. Olas**[3] (ID), **Bernd Mueller-Roeber**[1,3] (ID), **Mark Stitt**[1] (ID), **Christine A. Beveridge**[2] (ID) and **John E. Lunn**[1] (ID)

[1]Max Planck Institute of Molecular Plant Physiology, Potsdam-Golm 14476, Germany; [2]School of Biological Sciences, The University of Queensland, St Lucia, QLD 4072, Australia; [3]Institute of Biochemistry and Biology, University of Potsdam, Karl-Liebknecht-Straße 24-25, Haus 20, Potsdam 14476, Germany

Authors for correspondence:
Franziska Fichtner
Email: f.fichtner@uq.edu.au

John E. Lunn
Email: lunn@mpimp-golm.mpg.de

Summary

- Trehalose 6-phosphate (Tre6P) is a sucrose signalling metabolite that has been implicated in regulation of shoot branching, but its precise role is not understood.
- We expressed tagged forms of TREHALOSE-6-PHOSPHATE SYNTHASE1 (TPS1) to determine where Tre6P is synthesized in arabidopsis (*Arabidopsis thaliana*), and investigated the impact of localized changes in Tre6P levels, in axillary buds or vascular tissues, on shoot branching in wild-type and branching mutant backgrounds.
- TPS1 is expressed in axillary buds and the subtending vasculature, as well as in the leaf and stem vasculature. Expression of a heterologous Tre6P phosphatase (TPP) to lower Tre6P in axillary buds strongly delayed bud outgrowth in long days and inhibited branching in short days. TPP expression in the vasculature also delayed lateral bud outgrowth and decreased branching. Increased Tre6P in the vasculature enhanced branching and was accompanied by higher expression of *FLOWERING LOCUS T* (*FT*) and upregulation of sucrose transporters. Increased vascular Tre6P levels enhanced branching in *branched1* but not in *ft* mutant backgrounds.
- These results provide direct genetic evidence of a local role for Tre6P in regulation of axillary bud outgrowth within the buds themselves, and also connect Tre6P with systemic regulation of shoot branching via FT.

Introduction

Shoot architecture is a highly plastic trait that influences plant fitness in the wild and crop plant productivity (Patrick & Colyvas, 2014). In many plants, the shoot apex inhibits the outgrowth of axillary (lateral) buds, prioritizing allocation of resources towards growth of the main stem. This phenomenon is known as apical dominance. Removal of the shoot apex, by herbivory or pruning, leads to the release of dormancy in axillary buds allowing them to grow out to form new branches. Since the 1930s, there has been a general consensus that auxin is the main signal responsible for apical dominance (Barbier *et al.*, 2019). Auxin is produced in the young leaves at the shoot tip and transported down towards the roots, inhibiting the outgrowth of axillary buds along the shoot (Dun *et al.*, 2009; Muller & Leyser, 2011; Brewer *et al.*, 2013). Although the polar auxin stream in the stem inhibits bud outgrowth, auxin derived from the shoot tip does not itself move into axillary buds. Instead it acts via two other phytohormones: strigolactones and cytokinins (Wickson & Thimann, 1958; Sachs & Thimann, 1967; Gomez-Roldan *et al.*, 2008; Umehara *et al.*, 2008), which have antagonistic effects on axillary buds (Brewer *et al.*, 2009; Ferguson & Beveridge, 2009; Dun *et al.*, 2012, 2013). Auxin enhances synthesis of strigolactones, which inhibit

axillary bud growth (Shimizu-Sato *et al.*, 2009; Domagalska and Leyser, 2011), partly via induction of the BRANCHED1 (BRC1) transcription factor, which is a repressor of branching (Aguilar-Martinez *et al.*, 2007; Dun *et al.*, 2009, 2012; Braun *et al.*, 2012). Conversely, auxin inhibits biosynthesis of cytokinins, which promote axillary bud outgrowth, in part by repression of *BRC1* expression (Braun *et al.*, 2012; Dun *et al.*, 2012). A more recent concept is the auxin canalization model. This postulates that the inability of axillary buds to export auxin produced in the bud is responsible for their dormancy, and that outgrowth occurs when the buds are able to establish their own polar auxin stream (Prusinkiewicz *et al.*, 2009; Muller & Leyser, 2011).

Although these phytohormones undoubtedly play a major role in regulation of shoot branching, decapitation experiments in garden pea (*Pisum sativum*) questioned their involvement in the initial outgrowth of axillary buds. Decapitation leads to changes in the sucrose supply at the level of the lower buds that are highly correlated with the timing of bud outgrowth (Mason *et al.*, 2014; Fichtner *et al.*, 2017). Increasing the sucrose supply to axillary buds by feeding sucrose exogenously or removing the youngest growing leaves (i.e. competing sinks) also triggered bud growth, even when the shoot apex itself was left intact to maintain polar

auxin flow (Mason *et al.*, 2014). Exogenous sucrose also triggered bud outgrowth in stem explants from pea, rose (*Rosa hybrida*) and arabidopsis (Barbier *et al.*, 2015b; Fichtner *et al.*, 2017), even in the presence of auxin (Bertheloot *et al.*, 2020). These findings provide direct evidence that changes in sucrose supply are the initial signal that releases bud dormancy after decapitation. Observations in other species are consistent with sucrose supply playing an important role in shoot branching (Kebrom *et al.*, 2010, 2012; Barbier *et al.*, 2015a, 2019b; Martín-Fontecha *et al.*, 2018), with dormant buds displaying a carbon starvation-like transcript profile (Tarancón *et al.*, 2017).

Trehalose 6-phosphate (Tre6P) is an essential signal metabolite in plants (Fichtner & Lunn, In press). The sucrose-Tre6P nexus model proposes that Tre6P signals the availability of sucrose (Lunn *et al.*, 2006) and acts as a negative feedback regulator of sucrose levels (Yadav *et al.*, 2014; Figueroa & Lunn, 2016). Tre6P is synthesized by Tre6P synthase (TPS), and dephosphorylated by Tre6P phosphatase (TPP). In arabidopsis, *TPS* and *TPP* gene transcripts have been detected in meristems and axillary buds, and the expression of many of these genes is influenced by sugars and phytohormones (Osuna *et al.*, 2007; Ramon *et al.*, 2009; Yadav *et al.*, 2014). Transcriptomic and mutant studies have implicated Tre6P in shoot and inflorescence branching in arabidopsis (Schluepmann *et al.*, 2003), and other species (Kebrom & Mullet, 2016). In maize (*Zea mays*), inflorescence branching is increased by mutations in two *TPP* genes – *ZmRAMOSA3* and *ZmTPP4* – that disrupt putative Tre6P signalling functions (Satoh-Nagasawa *et al.*, 2006; Claeys *et al.*, 2019).

We recently demonstrated that Tre6P rapidly accumulates in pea axillary buds after decapitation, and that the rise in bud Tre6P levels following decapitation is dependent on sucrose (Fichtner *et al.*, 2017). Although the rise in bud Tre6P levels coincided with the onset of bud outgrowth, its physiological significance is not yet known (Fichtner *et al.*, 2017). Tre6P content is known to increase in sink tissues that accumulate sucrose following manipulation of sink capacity (Radchuk *et al.*, 2010; Nunes *et al.*, 2013). In maize, *grassy tillers1* and *teosinte branched1* mutants are highly branched because the tiller buds fail to establish dormancy, and this trait is associated with tiller buds having elevated levels of Tre6P (Dong *et al.*, 2019).

There is circumstantial evidence that Tre6P might also have a more remote influence on axillary buds and shoot branching, in particular via effects on the expression of the florigenic protein FLOWERING LOCUS T (FT; Wahl *et al.*, 2013). FT is synthesized in the phloem companion cells in leaves and moves in the phloem sieve elements to the shoot apical meristem (SAM), where it promotes the floral transition (Turck *et al.*, 2008). In arabidopsis, FT and its homologue, TWIN SISTER OF FT (TSF), interact with the branching repressor BRC1 in axillary buds (Niwa *et al.*, 2013). In rice (*Oryza sativa*), a homologue of FT regulates tillering (Tsuji *et al.*, 2015), and increased branching has been linked to upregulation of FT in tomato (*Solanum lycopersicum*) and tobacco (*Nicotiana tabacum*) (Li *et al.*, 2015; Weng *et al.*, 2016). In pea, one FT homologue, GIGAS, has also been implicated in the regulation of bud outgrowth (Beveridge & Murfet, 1996; Hecht *et al.*, 2011).

We hypothesize that Tre6P influences shoot branching in multiple ways, acting both locally within axillary buds and more remotely in the phloem-loading zone of leaves, potentially linking axillary bud outgrowth to the local availability of sucrose as well as the overall C-status of the plant. The aims of this study were to define where Tre6P acts in regulation of axillary bud outgrowth and to identify interactions with other signalling pathways that affect shoot branching. We used tissue-specific promoters to bring about localized changes in Tre6P levels in arabidopsis, and investigated the impact of these changes on shoot branching. We demonstrate that Tre6P plays a central role in the release of axillary bud dormancy to form new shoot branches.

Materials and Methods

Materials

Arabidopsis thaliana (L.) Heynh. accession Columbia-0 (Col-0) seeds were from an in-house collection. The *tps1-1* lines complemented with β-GLUCURONIDASE- or GFP-tagged forms of TREHALOSE-6-PHOSPHATE SYNTHASE1 (TPS1) or with the *Escherichia coli* TPS (OtsA) were those described in Fichtner *et al.* (2020).

Molecular cloning

The *BRC1* (*BRANCHED1*, At3g18550) promoter was obtained by PCR amplification of a 1-kbp genomic region upstream of the start codon. The *GLYCINE-DECARBOXYLASE P-SUBUNIT A* (*GLDPA*) promoter from *Flaveria trinervia* was amplified as a 1.5-kbp fragment from the the FtGLDPA5′-pBI121 plasmid (see Engelmann *et al.*, 2008). Promoter sequences were integrated into pGreenII plasmids (www.pgreen.ac.uk; Hellens *et al.*, 2000) containing the *Agrobacterium tumefaciens* octopine synthase terminator. The *E. coli* (strain K12) *otsA* gene was amplified from genomic DNA and the *CeTPP/GOB-1* coding sequence, codon-optimized for expression in arabidopsis, was synthesized and cloned by GenScript (www.genscript.com) and sub-cloned into the pGreenII plasmid.

Arabidopsis transformation

Gene constructs were introduced into arabidopsis Col-0 by *Agrobacterium tumefaciens* mediated floral dipping (Clough & Bent, 1998). Primary transformants were selected by spraying with 0.05% (v/v) glufosinate. Lines that showed a 3 : 1 segregation of resistant : susceptible individuals in the T₂ generation, indicating a single transgenic locus, were chosen for further propagation. T₃ progeny from such lines were screened by glufosinate selection to identify homozygous lines.

Plant growth conditions

Seeds were stratified for 3 d at 4°C and grown for 7 d on solid half-strength MS plates (Murashige & Skoog, 1962) and then transferred to a 1 : 1 mixture of vermiculite and soil (Stender,

www.stender.de). Plants under fluorescent lighting (Annunziata et al., 2017), with 8-h, 16-h or 18-h photoperiods, 150 µmol m^{-2} s^{-1} irradiance and day : night temperatures of 22°C : 18°C. Unless stated otherwise, plants were harvested 10 h after dawn (ZT10). The age of the plants at harvest is indicated for each individual experiment. Bud enriched material was obtained from rosettes by removing all leaves as well as the hypocotyl, leaving only the inner stem regions and shoot apex. For vascular enriched material, the leaf mid-veins of three plants were dissected and pooled. Dormant axillary buds were collected from 15 plants 1 wk after bolting.

Phenotyping

Flowering time was determined as total leaf number (rosette + cauline leaves). Rosette and cauline leaves were counted separately, and the rosette leaf number was used to determine primary rosette (RI) branch (Fig. 1i) number per leaf. Shoots (≥ 0.5 cm) were counted either when they had finished flowering and fully senesced or every 2 or 3 d after bolting. See Fig. 1(i) for branch nomenclature.

Microscopy

β-Glucuronidase (GUS) reporter assay Plants were placed in β-glucuronidase (GUS) staining solution (50 mM sodium-phosphate buffer (pH 7), 5 mM K$_3$[Fe(CN)$_6$], 5 mM K$_4$[Fe(CN)$_6$], and 1 mM 5-bromo-4-chloro-3-indolyl-β-D-glucuronic acid (X-Gluc). After incubation at 37°C in the dark overnight, the tissue was destained by washing several times with 70% (v/v) ethanol. Meristems were harvested, fixed, embedded in wax, sectioned and imaged under an Olympus BX-51 Epi-Fluorescence Microscope (www.olympus-lifescience.com) as described in Olas et al. (2019). Nonsectioned plant material was imaged under a Leica Stereomicroscope MZ12.5 (Leica Biosystems; www.leicabiosystems.com).

GFP-reporter lines GREEN FLUORESCENT PROTEIN (GFP) expression was detected using a Leica TCS SP8 spectral laser scanning confocal motorized microscope. Overlays were done using the image processing package Fiji for ImageJ (https://fiji.sc/).

Immunoblotting

Expression of heterologous proteins was confirmed by immunoblotting as described previously (Martins et al., 2013). The following primary antibodies were used: (1) rabbit anti-OtsA (Martins et al., 2013; 1 : 3000 dilution) or (2) rabbit anti-CeTPP kindly provided by Dr Carlos Figueroa (MPI-MP, Potsdam-Golm, Germany; 1 : 4000 dilution).

Metabolite analysis

Frozen plant tissue was ground to a fine powder at liquid nitrogen temperature and water-soluble metabolites were extracted as described in Lunn et al. (2006). Tre6P, other phosphorylated intermediates and organic acids were measured by anion-exchange high-performance liquid chromatography (HPLC) coupled to tandem mass spectrometry (Lunn et al., 2006), with modifications as described in Figueroa et al. (2016). Sucrose was measured enzymatically (Stitt et al., 1989).

Gene expression analysis

RNA was extracted using an RNeasy Plant Mini Kit (Qiagen; www.qiagen.com). For absolute quantification of transcripts, ArrayControl RNA Spikes (Applied Biosystems; www.thermofisher.com/applied/biosystems) were added before RNA extraction and cDNA synthesis (Flis et al., 2015). Contaminating DNA was removed using a Turbo DNA-free kit, and reverse transcription was performed using a SuperScript IV First-Standard Synthesis System Kit (Invitrogen; www.thermofisher.com/Invitrogen). The PCR mix was prepared using Power SYBR Green PCR Master Mix (Applied Biosystems), and quantitative reverse transcription polymerase chain reaction (qRT-PCR) was performed in a 384-well microplate using an ABI Prism 7900 HT sequence detection system (Applied Biosystems). Transcript abundance was calculated as described in Flis et al. (2015), using spike numbers 1 to 7. Primers used for spike analysis and qRT-PCR are given in Supporting Information Table S1. Gene expression analysis was also performed as described in Barbier et al. (2019a). Complementary DNA (cDNA) was synthesized by reverse-transcription using an iScript™ cDNA Synthesis Kit (Bio-Rad; www.biorad.com). Quantitative real-time PCR was performed using a SensiFAST™ SYBR® No-ROX Kit (Bioline; www.bioline.com). Fluorescence was monitored with a CFX384 thermal cycler (Bio-Rad). Gene expression was calculated using the ΔΔCt method corrected by the primer efficiency, and *TUBULIN3* and *ACTIN* (combination of *ACT2, ACT7* and *ACT8*; Table S1) were used for normalization.

Statistical analysis

Data plotting and statistical analysis were performed using R Studio v.1.0.143 (www.rstudio.com) with R v.3.6.2 (https://cran.r-project.org/). Data were analysed using an analysis of variance (ANOVA) based *post hoc* comparison of means test using the multiple comparison Fisher's least significant difference (LSD) test. Figures containing micrographs and other images were compiled using Adobe Illustrator, Microsoft PowerPoint 2010 or ImageJ software (https://imagej.nih.gov/ij/).

Results

Localization and function of TPS1 in arabidopsis axillary buds

TPS1 is the predominant enzymatic source of Tre6P in arabidopsis (Delorge et al., 2015). To assess the potential for Tre6P synthesis in axillary buds, we complemented the arabidopsis *tps1-1* null mutant, which is unable to complete embryogenesis
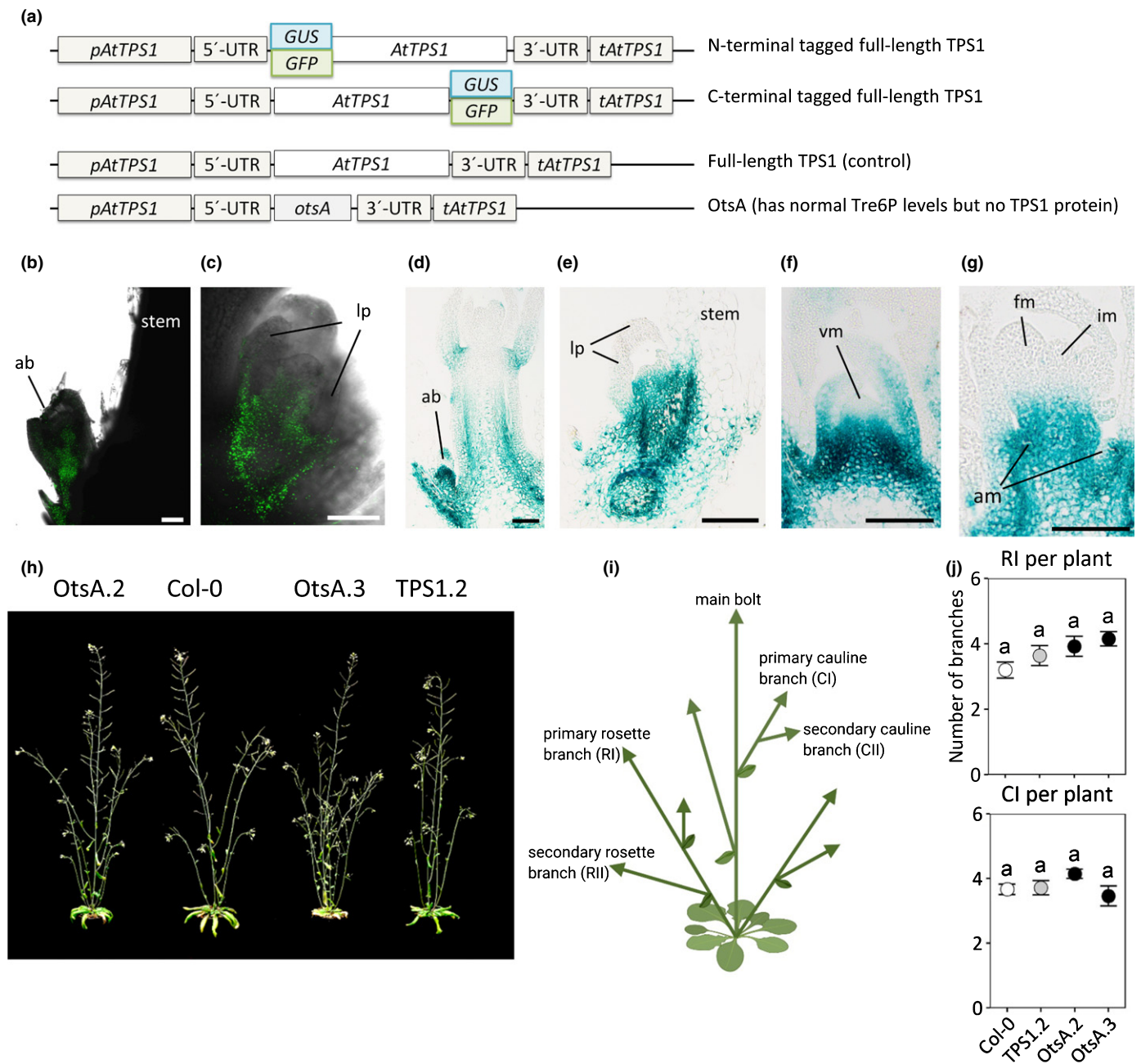
Fig. 1 TPS1 localization and trehalose 6-phosphate (Tre6P) synthesis during bud development. (a) *TPS1* constructs are derived from the arabidopsis *TPS1* (At1g78580) genomic locus, including the native promoter (*pAtTPS1*) and terminator (*tAtTPS1*) regions (Fichtner *et al.*, 2020). TPS1 fusion proteins tagged with the GREEN FLUORESCENT PROTEIN (GFP; green box) or the β-GLUCURONIDASE (GUS; blue box) were used to analyse the TPS1 expression pattern. A construct encoding the full-length TPS1 protein was used as a control together with a construct expressing only the heterologous TPS from *Escherichia coli* (OtsA) under the control of the *TPS1* gene regulatory elements (*pAtTPS1* and *tAtTPS1*). Plants were grown in 16-h photoperiods and stained for GUS activity or examined for GFP. (b, c) TPS1-GFP fusion protein expression in axillary buds. (d, e) TPS1-GUS fusion protein expression in rosette axillary buds. TPS1-GUS fusion protein expression in (f) vegetative and (g) inflorescence and floral meristems. (h) Visual phenotype of wild-type Col-0 plants and full-length TPS1 as well as OtsA complemented *tps1-1* plants photographed at 44 d after sowing (DAS). (i) Schematic representation of arabidopsis branching structure and nomenclature. (j) Primary rosette (RI) branches or cauline (CI) branches per plant (length ≥ 0.5 cm) were counted at the end of the plant's life cycle. Data are presented as mean ± SEM (*n* = 13–15). Wild-type and transgenic lines complementing the *tps 1-1* mutant are represented by different symbol colours: Col-0 (white), full length TPS1 (grey), OtsA (black). Letters indicate significant differences between treatments according to one-way ANOVA with *post hoc* LSD testing (*P* ≤ 0.05). vm, vegetative meristem; im, inflorescence meristem; fm, floral meristem; am, axillary meristem; ab, axillary bud; lp, leaf primordia; bars, 100 μm.

(Eastmond *et al.*, 2002), with constructs encoding full-length TPS1 proteins tagged at either the N- or C-terminus with GUS or GFP (Fig. 1a). Expression of the TPS fusion proteins was

under the control of the endogenous *TPS1* promoter and other potential regulatory elements from the *TPS1* genomic locus, and the complemented lines showed normal embryonic and post-

embryonic growth (Fichtner *et al.*, 2020; Fig. 1a). GUS/GFP-tagged TPS1 was detected in axillary buds (Fig. 1b–e), with strong expression also in the subtending vasculature, but there was little or no expression in leaf primordia or the central meristematic zone of the axillary buds (Fig. 1b–e). This was similar to the expression pattern of TPS1 in the main shoot apex. Before bolting, TPS1 was detected in the flanks and rib zone of the SAM, and in the proto-vasculature subtending the SAM (Fig. 1e), consistent with previous studies of the same reporter lines (Fichtner *et al.*, 2020). Similarly, TPS1 was present in the vasculature subtending the inflorescence SAM as well as in cauline axillary meristems (Fig. 1g).

To investigate the dependence of shoot branching in arabidopsis on TPS1, we analysed shoot branching patterns in two independent transgenic lines in the *tps1-1* null mutant background, in which loss of TPS1 had been complemented by expression of the OtsA under the control of the *TPS1* promoter and other *TPS1* gene regulatory elements (Fig. 1a). These lines have no detectable TPS1 protein but wild-type levels of Tre6P (Fichtner *et al.*, 2020). Both OtsA-complemented lines had the same number of RI and cauline (CI) branches as wild-type plants and *TPS1*-complemented control plants, showing that Tre6P, rather than the TPS1 protein *per se*, is a key factor in regulation of shoot branching (Fig. 1h,i).

Together, these results indicate that there is the enzymatic capacity for Tre6P synthesis in axillary meristems and buds, and that replacement of the Tre6P-synthesizing function of TPS1 by OtsA is sufficient to restore wild-type patterns of shoot branching in the *tps1-1* mutant background.

Expression of a heterologous TPP in axillary buds supresses branching

To determine whether Tre6P is required for release of axillary bud dormancy and outgrowth into new shoots, we expressed a heterologous TPP in axillary buds to lower their Tre6P content. We used the promoter of the arabidopsis *BRC1* gene, which is predominantly expressed in axillary buds (Aguilar-Martinez *et al.*, 2007), to drive expression of a heterologous TPP from *Caenorhabditis elegans* (CeTPP), whose K_m for Tre6P (0.1–0.15 mM; Kormish & McGhee, 2005) is in a similar range to estimates of *in vivo* Tre6P concentrations in plants (Martins *et al.*, 2013). We also generated several independent GUS and GFP reporter lines to confirm the expression pattern mediated by the *BRC1* promoter.

In the inflorescence apex, *pBRC1*-driven GUS expression was visible in axillary meristems and in the epidermis of young leaves (Fig. 2a shows representative images from several independent lines), consistent with the predominant expression in axillary buds described previously (Aguilar-Martinez *et al.*, 2007). Upon bolting, GUS expression was visible in axillary meristems of cauline leaves as well as in axillary buds of rosette leaves (Fig. 2a). Likewise, GFP fluorescence in *pBRC1:GFP* lines was detected in axillary buds (Fig. S1a). To confirm transgene expression in the *pBRC1* lines, mature axillary buds and fully expanded leaves were harvested from wild-type Col-0,

pBRC1:GUS and *pBRC1:CeTPP* lines at 1 wk after bolting for immunoblot analysis (Fig. 2b). In both of the *pBRC1:CeTPP* lines, an immunoreactive protein of the expected size of CeTPP (51 kDa) was detected only in the axillary bud material, with no detectable CeTPP protein in fully expanded leaf tissue (Fig. 2b). This confirms specific expression in mature axillary buds in these lines.

We also measured Tre6P and sucrose levels in rosette cores, enriched in axillary meristems and buds, at 21 d after sowing (DAS), when the plants had undergone the floral transition and produced axillary meristems, and at 31 DAS, when axillary buds had formed. The level of Tre6P was significantly decreased in *pBRC1:CeTPP* line #8 at 21 DAS, while sucrose was significantly increased in *pBRC1:CeTPP* line #11 at 21 DAS (Fig. 2c). The Tre6P : sucrose ratio was significantly decreased in *pBRC1: CeTPP* line #8 at 21 DAS and in *pBRC1:CeTPP* line #11 at both time points (Fig. 2c,d).

The *pBRC1:CeTPP* plants with lower levels of Tre6P in axillary buds did not show any obvious changes in their vegetative growth pattern (Fig. S2). Similarly, flowering time and final RI branch number were unchanged (Figs 2e,f, S3a). However, when branching was scored in short-day conditions (8-h photoperiod), the *pBRC1:CeTPP* lines had fewer RI branches than the controls (Fig. 2g). We also analysed the difference in bud outgrowth by monitoring RI branch emergence over time in a 16-h photoperiod. Since independent lines showed consistent phenotypes, we focussed on a single line (*pBRC1:CeTPP* line #11) that showed the strongest accumulation of CeTPP protein. The emergence of RI branches was strongly delayed in the *pBRC1:CeTPP* plants, with the first appearance of RI branches occurring *c.* 8 d later than in the controls. The emergence of further RI branches was also noticeably slower in the *pBRC1:CeTPP* plants. As seen before, the final number of RI branches was the same in *pBRC1: CeTPP* and control plants (Fig. 2f,h), indicating that lowering bud Tre6P levels delays the initiation and rate of bud outgrowth, but does not affect the number of buds that eventually do form RI branches in long days. However, lowering Tre6P in axillary buds in short-day (i.e. carbon limiting) conditions severely decreased RI branching (Fig. 2g).

Tre6P levels in the vasculature affect shoot branching in arabidopsis

In arabidopsis leaves, the leaf vasculature is a major site of TPS1 expression, and by implication Tre6P synthesis and signalling (Fig. 1; Fichtner *et al.*, 2020). Arabidopsis is an apoplastic phloem loading species, in which sucrose is released from phloem parenchyma cells into the apoplast via SUCROSE WILL EVENTUALLY BE EXPORTED type sucrose effluxers (SWEET11 and SWEET12) and then actively taken up into the companion cell-sieve element complex by the SUT1/SUC2 sucrose-H^+ symporter (Lalonde *et al.*, 2003; Baker *et al.*, 2012; Chen *et al.*, 2012; Eom *et al.*, 2015; Zakhartsev *et al.*, 2016). To investigate the potential of Tre6P synthesis in the vasculature to influence shoot branching, we modified Tre6P levels preferentially in vascular tissues. We used the promoter of the *F. trinervia*
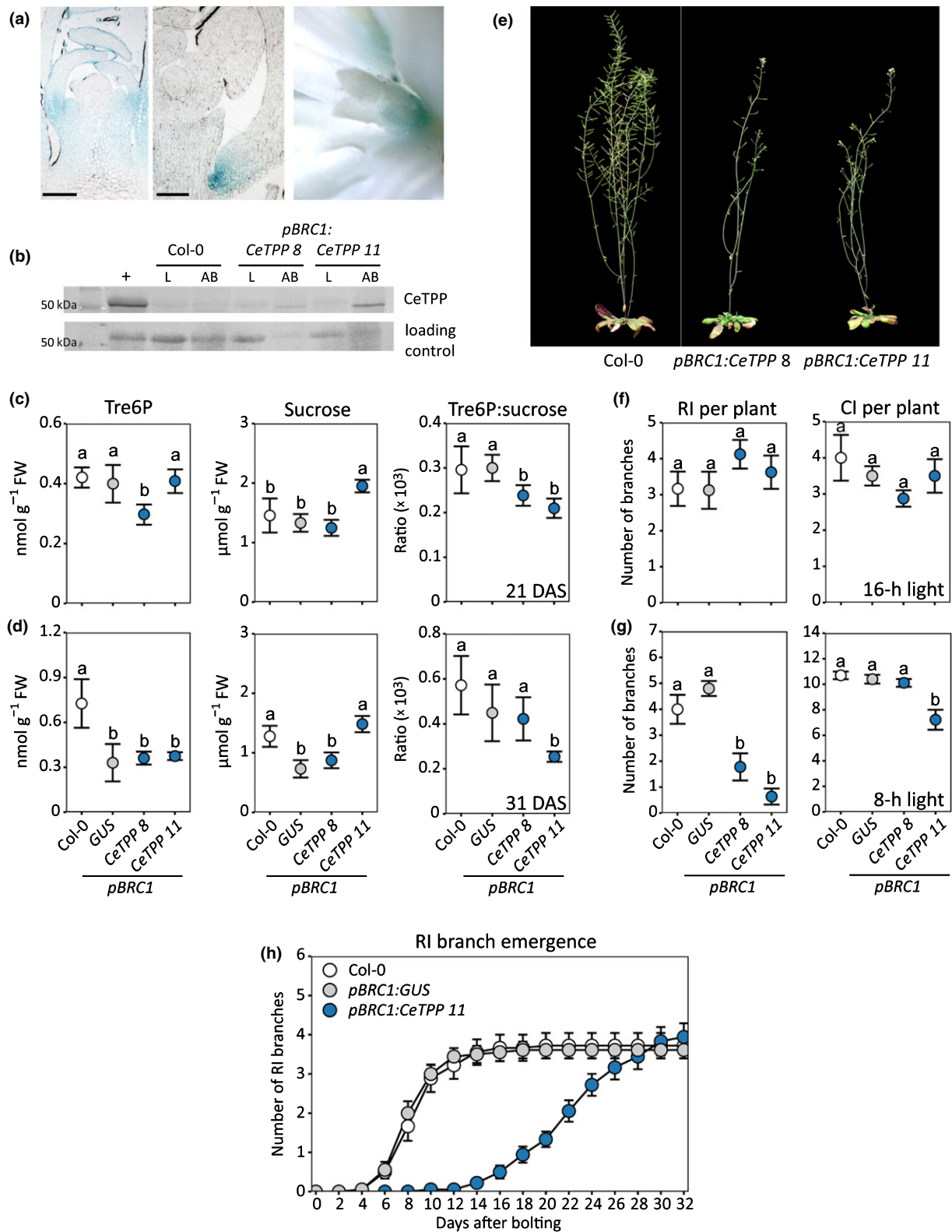
GLDPA gene to drive specific expression of *otsA* or *CeTPP* to increase or decrease Tre6P, respectively, in vascular tissues of arabidopsis. The *GLDPA* promoter had previously been reported to drive specific expression in the vasculature in arabidopsis

(Engelmann *et al.*, 2008; Wiludda *et al.*, 2012; Aubry *et al.*, 2014). We also generated *pGLDPA:GUS* and *pGLDPA:GFP* reporter lines to verify the expression pattern of the *GLDPA* promoter in arabidopsis. For comparison, we expressed *otsA* under

Fig. 2 Overexpression of TPP in axillary buds of arabidopsis. The arabidopsis *BRANCHED1* promoter (*pBRC1*) was used to drive specific expression in axillary buds. (a) The *β-GLUCURONIDASE* (*GUS*) reporter gene was expressed in arabidopsis Col-0 plants under the control of the *pBRC1* promoter and GUS activity was visualized in inflorescence meristems and dormant axillary buds. Bars, 200 µM. (b) Wild-type Col-0 and transgenic *pBRC1:GUS*, or *pBRC1:CeTPP* (*Caenorhabditis elegans GOB1*) lines were grown in a 16-h photoperiod. Leaves (L) and axillary buds (AB) were harvested around ZT10 for immunoblotting to detect expression of heterologous CeTPP proteins. Parallel samples of rosette cores were harvested at ZT10 from plants at (c) 21 and (d) 31 d after sowing (DAS) for metabolite analyses. Data are presented as mean ± SD (*n* = 4). (e) Visual phenotypes of *pBRC1:CeTPP* arabidopsis plants photographed *c*.18 d after bolting. Primary rosette (RI) or cauline (CI) branches were counted (f) in 16-h or (g) 8-h photoperiods. (h) The number of RI branches (length ≥ 0.5 cm) per plant was counted at 2-d intervals after bolting in a 16-h photoperiod. Branches (length ≥ 0.5 cm) were counted at the end of the plant's life cycle. Data are shown as mean ± SEM (*n* = 8–18). Wild-type and transgenic lines expressing heterologous proteins are represented by different symbol colours: Col-0 (white), GUS (grey), and CeTPP (blue). Letters indicate significant differences between treatments according to one-way ANOVA with *post hoc* LSD testing (*P* ≤ 0.05). +, positive control.

the control of the constitutive Cauliflower Mosaic Virus *35S* promoter, as this had previously been reported to give a bushy phenotype (Schluepmann *et al.*, 2003).

GUS activity was localized to the vascular tissue in the leaves and petioles of *pGLDPA:GUS* lines (Figs 3a, S1b), with transverse sections showing staining throughout the vascular bundles (xylem and phloem tissues; Fig. 3a shows representative images from several independent lines). There was expression in the vasculature subtending dormant axillary buds, with a sharp boundary at the base of the bud and no detectable expression in the bud itself (Fig. 3a). Expression was also seen in the vasculature subtending vegetative and inflorescence SAMs but not in the SAM itself (Fig. S1c). Except for the background signal generated by the autofluorescence of the chloroplasts, no GFP signal was detected outside of the vasculature in *pGLDPA:GFP* lines (Fig. S1d). To confirm correct transgene expression, immunoblot analyses were performed in extracts of: (1) whole leaves and (2) dissected mid-veins, the latter being substantially enriched in vascular tissue. The abundance of the OtsA protein in vasculature-enriched extracts from the *p35S:otsA* plants was similar to that in whole-leaf extracts (Fig. 3b), indicating expression at a similar level throughout the leaf. By contrast, OtsA and CeTPP were more abundant in the vasculature-enriched samples from two independent *pGLDPA:otsA* and *pGLDPA:CeTPP* lines, respectively, than in the corresponding whole-leaf extracts (Fig. 3b). Together, the GUS/GFP reporter lines and the immunoblotting data confirm that the *GLDPA* promoter drives vasculature specific expression of heterologous proteins in arabidopsis.

Tre6P was significantly increased in rosettes of the *p35S:otsA* plants (five-fold) as well as in both *pGLDPA:otsA* lines (two-fold) compared to wild-type Col-0 and control plants (Fig. 3c). The *p35S:otsA* and *pGLDPA:otsA* lines had lower sucrose levels, resulting in a significantly increased Tre6P : sucrose ratio in the *p35S:otsA* (10-fold) plants and in both *pGLDPA:otsA* lines (three-fold; Fig. 3c). The *pGLDPA:CeTPP* lines had significantly higher rosette sucrose levels (Fig. 3c). In vasculature-enriched samples, Tre6P levels were significantly higher than wild-type in *p35S:otsA* and *pGLDPA:otsA* lines, while the *pGLDPA:CeTPP* lines had significantly less Tre6P (30–40% lower than wild-type; Fig. 3d). Similarly, the Tre6P : sucrose ratio was increased (two-fold) in *p35S:otsA* and *pGLDPA:otsA* lines and decreased (by *c*. 50%) in *pGLDPA:CeTPP* plants, compared to wild-type and *pGLDPA:GUS* control plants (Fig. 3d).

Tre6P has been implicated in transcriptional regulation of *SWEET* expression in sorghum and maize (Kebrom & Mullet,

2016; Bledsoe *et al.*, 2017; Oszvald *et al.*, 2018). Therefore, we measured the transcript abundance of *SWEET* and other sucrose transporter (*SUT/SUC*) genes to investigate the potential impact of increased Tre6P levels in the vasculature on phloem loading of sucrose. Expression of *otsA* was confirmed in both *pGLDPA:otsA* lines, with no *otsA* transcript being detected in the *pGLDPA:GUS* control line (Fig. 3e). *SUT1/SUC2* transcript abundance was the same in all genotypes, but the two *pGLDPA:otsA* lines had 1.5–1.8 times higher levels of *SWEET11* and *SWEET12* transcripts (Fig. 3f).

To follow up these preliminary observations, we measured the transcript abundance of all four *SWEET* genes (*SWEET11–SWEET14*) that are known to encode plasmalemma sucrose efflux carriers (Chen *et al.*, 2012; Kanno *et al.*, 2016) in leaf 6 (a fully expanded source leaf) and in the rosette core (enriched in axillary buds) from *pGLDPA:otsA* (line #5) and control *pGLDPA:GUS* plants at 2 d after bolting (Fig. 4a). *SWEET11* and *SWEET12* were upregulated *c*. 2.5-fold in the *pGLDPA:otsA* plants (Fig. 4a), consistent with our previous results based on whole rosette measurements that were performed at a different biological age and time of the day (Fig. 3f). *SWEET13* was also significantly upregulated (three-fold), but *SWEET14* transcripts were not detected (Fig. 4a). In contrast to leaves, there was no upregulation of *SWEET11* and *SWEET12* in axillary bud enriched rosette cores but transcripts of *SWEET13* and *SWEET14* were three-times more abundant in rosette cores from the *pGLDPA:otsA* plants than in the controls (Fig. 4a). We confirmed these results using the *p35:otsA* line as well as the other independent *pGLDPA:otsA* line #1 in an independent experiment (Fig. S4). Both lines showed a two-fold upregulation of *SWEET11*, *SWEET12* and *SWEET13* in leaves and a five- to seven-fold upregulation of *SWEET13* in rosette cores (Fig. S4, note *SWEET14* transcripts were not detected). By contrast, the *pGLDPA:CeTPP* line #4 showed a two-fold reduction in *SUC2*, *SWEET11*, *SWEET12* and *SWEET13* transcript levels in leaves, but no difference in expression in rosette cores.

As previously observed (Schluepmann *et al.*, 2003; Yadav *et al.*, 2014), the *p35S:otsA* plants had much smaller rosettes and darker green leaves than wild-type Col-0 plants (Fig. S5). Similarly, the *pGLDPA:otsA* lines had smaller rosettes than wild-type, although not as small as the *p35S:otsA* plants, whereas the *pGLDPA:CeTPP* lines had slightly bigger leaves than wild-type (Fig. S5).

In long-day conditions *p35S:otsA* and *pGLDPA:otsA* plants displayed increased shoot branching (Fig. 5a). On average, wild-type
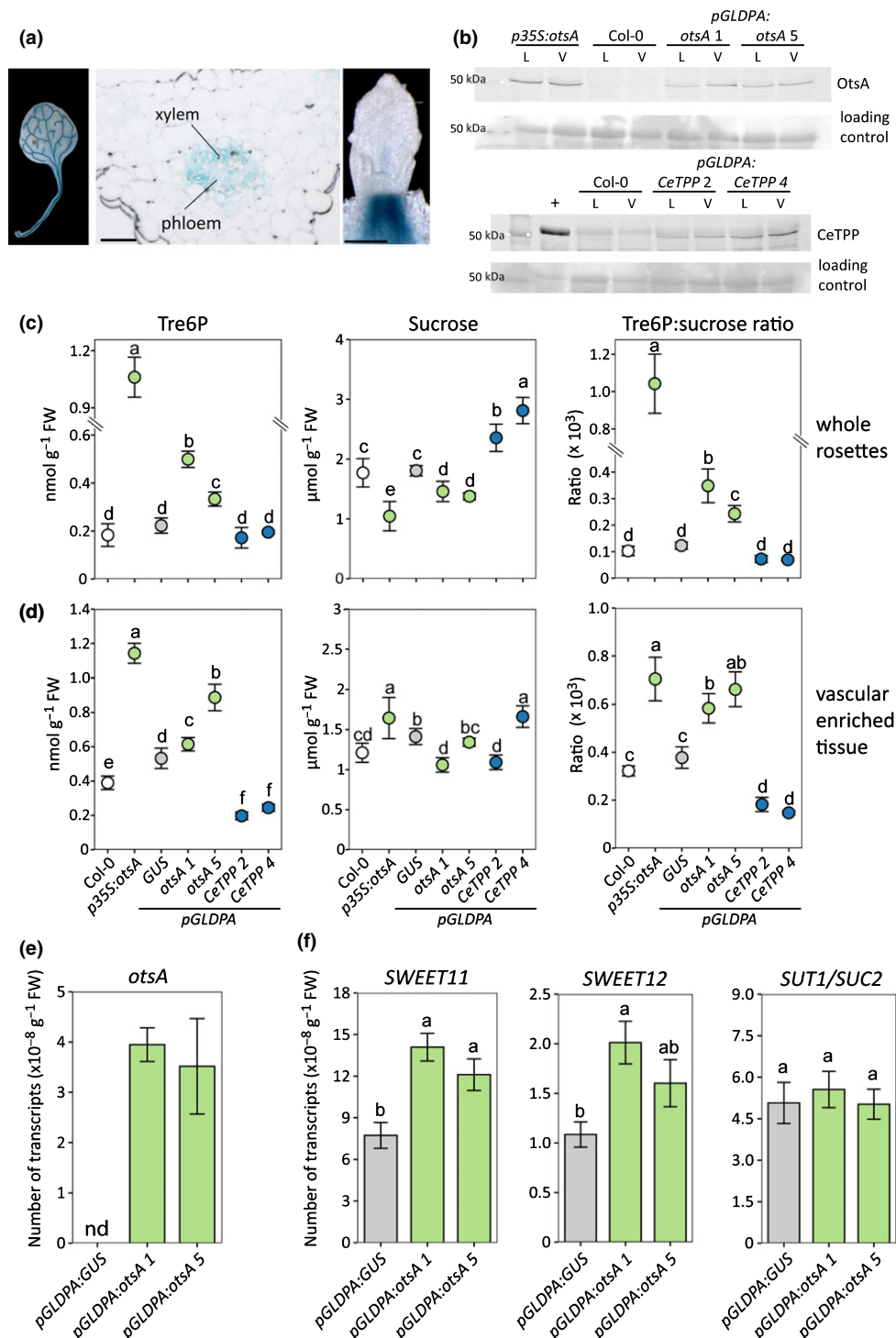
Fig. 3 Overexpression of TPS or TPP in the vasculature of arabidopsis. The *Flaveria trinervia GLYCINE-DECARBOXYLASE P-SUBUNIT A* promoter (*pGLDPA*) was used to drive specific expression in the vasculature of arabidopsis. (a) The *β-GLUCURONIDASE* (*GUS*) reporter was expressed in arabidopsis Col-0 plants under the control of *pGLDPA* and GUS activity was visualized in rosette leaves, transverse sections of the mid-vein region of fully expanded leaves and in dormant axillary buds. Bars, 100 μm. (b) Wild-type Col-0 and transgenic *p35S:otsA* (*Escherichia coli otsA*), *pGLDPA:GUS*, *pGLDPA:otsA* and *pGLDPA:CeTPP* (*Caenorhabditis elegans GOB1*) lines were grown in a 16-h photoperiod. Leaves (L) and vasculature-enriched (V) tissues were harvested at ZT10 from plants at 20 d after sowing (DAS) to detect expression of heterologous TPS (OtsA) or TPP (CeTPP) proteins by immunoblotting. Parallel samples of whole rosettes (c) or vasculature-enriched tissue (d) were collected for metabolite analyses. Data are presented as mean ± SD ($n = 4$). (e) Transcript abundance of the *otsA* gene in rosettes from plants grown under long-day conditions and harvested at ZT10 at 24 DAS. (f) Transcript abundance of *SUT1/SUC2*, *SWEET11* and *SWEET12* in the same samples as (e). Data are presented as mean ± SEM ($n = 4$ biological replicates). Wild-type and transgenic lines expressing heterologous proteins are represented by different symbol colours: Col-0 (white), GUS (grey), OtsA (green) and CeTPP (blue). Letters indicate significant differences between treatments according to one-way ANOVA with *post hoc* LSD testing ($P \leq 0.05$). +, positive control; nd, not detected.

Col-0 and control plants developed only two to three RI branches, while the *p35S:otsA* and *pGLDPA:otsA* lines had four to six RI branches (Fig. 5b). RI branch number in the *pGLDPA: CeTPP* lines was similar to wild-type Col-0 and control plants (Fig. 5b). In arabidopsis, an axillary bud develops in the axil of each rosette leaf. Therefore, the number of RI branches per plant is potentially influenced by the total number of rosette leaves. Leaf number also influences the overall photosynthetic capacity and potential sucrose supply of the plant. As total leaf number was decreased in the *p35S:otsA* and *pGLDPA:otsA* lines and increased in the *pGLDPA:CeTPP* lines (Fig. S3c), the total number of RI branches was also plotted on a per rosette leaf basis (RI per leaf). The *p35S:otsA* plants and both *pGLDPA:otsA* lines had twice as many RI branches per leaf as wild-type and control plants (Fig. 5b), whereas *pGLDPA:CeTPP* line #4 showed the opposite phenotype, with only half the wild-type number of RI per leaf (Fig. 5b). The stronger phenotype of *pGLDPA:CeTPP* line #4 compared to line #2 was consistent with the higher abundance of CeTPP protein in this line (Fig. 3b). In addition to the increase in RI branches, the *pGLDPA:otsA* lines also had a significantly increased ratio of secondary rosette (RII) to RI branches (RII : RI ratio; Fig. 5b), indicating that outgrowth of secondary buds was also stimulated in these plants. We also determined the
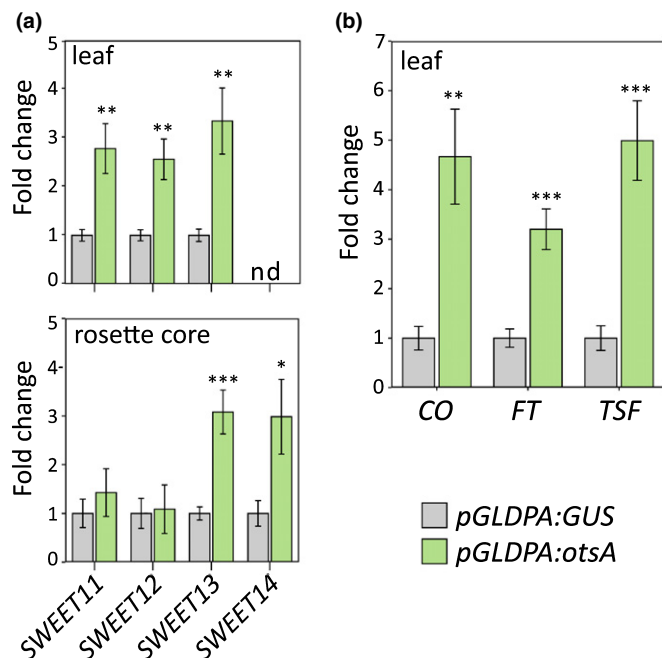
number of CI branches per plant. As the *pGLDPA:otsA* lines flowered earlier than the controls, they produced fewer CI branches, whereas the late flowering *pGLDPA:CeTPP* plants developed more CI branches (Fig. 5b).

Essentially the same effects on shoot branching and leaf number were observed in an independent experiment where the plants were grown in a slightly longer (18 h) photoperiod (Figs 5c, S4d). However, when grown in an 18-h photoperiod, total leaf number was similar for *pGLDPA:otsA* and control plants (Fig. S3d), and there were no differences in CI branch number, except for *pGLDPA:otsA* line #1 which had more CI branches due to formation of a second CI branch at some axils (Fig. S6).

The number of RI branches was also monitored over time in long-day grown plants and plotted against days after bolting. Initiation of new branches continued for longer in the *p35S:otsA* and *pGLDPA:otsA* (line #5) plants, so by the time the plants were fully senesced they had more RI branches per plant and RI branches per rosette leaf than the control plants (Fig. 5d). In the *pGLDPA:CeTPP* (line #4) plants, the emergence of lateral branches was slower than in the control plants (Fig. 5d). Similar results were obtained when 4-wk-old plants grown in short days (8-h photoperiod) were shifted to long-day conditions (16-h photoperiod) (Fig. S7). Initiation of new branches was faster in both *pGLDPA:otsA* lines, and they had more RI branches per plant and RI branches per rosette leaf than the control plants (Fig. S7b). By contrast, RI branch emergence was slower in both *pGLDPA:CeTPP* lines than in the control plants (Fig. S7b).

As flowering time and branching were affected in the *pGLDPA:otsA* plants with elevated Tre6P in the vasculature, we determined the expression levels of *FT* and *TSF* and *CONSTANS* (*CO*) (a key regulator of *FT* expression; Turck *et al.*, 2008). Transcript analysis was performed on the same RNA samples from leaf 6 harvested from *pGLDPA:otsA* and *pGLDPA:GUS* plants grown in a 16-h photoperiod as described earlier (Fig. 4b). Compared to the *pGLDPA:GUS* controls, the *pGLDPA:otsA* plants showed significantly increased expression of *CO* (4.5-fold), *FT* (three-fold) and *TSF* (five-fold) (Fig. 4b).
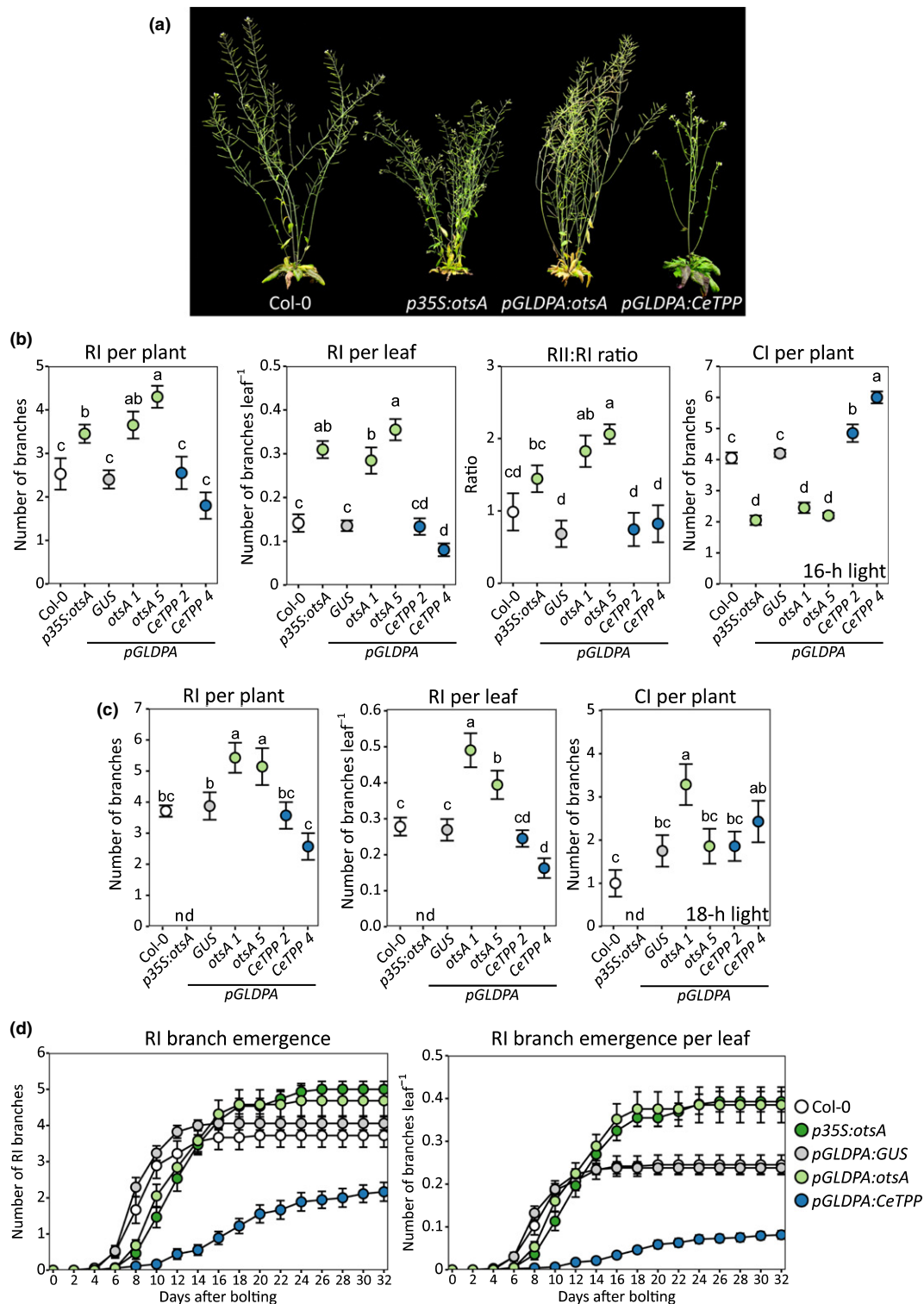
To summarize, the phenotypes of these transgenic lines demonstrate that: (1) higher Tre6P in the vasculature (*pGLDPA: otsA*) increased the final number of branches and was associated with upregulation of *SWEETs*, *CO*, *FT* and *TSF*; and (2) lowering Tre6P in the vasculature (*pGLDPA:CeTPP*) decreased final branch number and strongly delayed lateral bud outgrowth.

Rosette branch number correlates with Tre6P levels in the vasculature

We assessed the relationship between Tre6P, sucrose and the Tre6P : sucrose ratio in whole-rosette or vascular-enriched samples with the number of RI branches per plant and RI branches per leaf, using a Pearson's correlation analysis. Based on whole rosette measurements, we detected a significant negative correlation of sucrose levels with RI branches per plant and with RI branches per leaf (RI per plant: $r = -0.813$, $R^2 = 0.66$, $P = 0.026$; RI per leaf: $r = -0.855$, $R^2 = 0.732$, $P = 0.014$). The manipulation of Tre6P in the vasculature influences the rosette's sucrose

Fig. 4 Gene expression analyses in arabidopsis plants with altered trehalose 6-phosphate (Tre6P) levels in the vasculature. *pGLDPA:otsA* (green bars) and *pGLDPA:GUS* (grey bars) plants were grown in a 16-h photoperiod. Fully expanded leaves (leaf 6) and rosette cores were harvested at ZT14 on day 2 after bolting, i.e. after the floral transition but before axillary bud outgrowth. (a) Abundance of *SWEET11*, *SWEET12*, *SWEET13* and *SWEET14* transcripts. (b) Abundance of *CONSTANS* (*CO*), *FLOWERING LOCUS T* (*FT*) and *TWIN SISTER OF FLOWERING LOCUS T* (*TSF*). Data from the *pGLDPA:otsA* plants are expressed as fold-change with respect to the *pGLDPA:GUS* controls, and shown as mean ± SEM (*n* = 8 biological replicates). Asterisks show significant differences between the genotypes according to Student's *t*-test: *, $P < 0.05$; **, $P < 0.01$; ***, $P < 0.001$. nd, not detected.

Fig. 5 Axillary bud growth analysis in arabidopsis plants with altered trehalose 6-phosphate (Tre6P) levels in the vasculature. (a) Visual phenotypes of arabidopsis *p35S:otsA*, *pGLDPA:otsA* and *pGLDPA:CeTPP* plants, grown in a 16-h photoperiod and photographed at 56 d after sowing (DAS). Primary rosette (RI) branches per plant, RI branches per rosette leaf, ratio of secondary rosette (RII) and RI branches and primary cauline (CI) branches per plant were counted in (b) 16-h or (c) 18-h photoperiods. (d) The number of RI branches per plant and per leaf was counted at 2-d intervals after bolting of plants grown in a 16-h photoperiod (note the wild-type data are from plants grown under identical conditions and are the same as those shown in Fig. 2h). Branch number was scored by counting visible branches (length ≥ 0.5 cm). Data are shown as mean ± SEM (*n* = 8–20). Wild-type and transgenic lines expressing heterologous proteins are represented by different symbol colours: Col-0 (white), GUS (grey), OtsA (green) and CeTPP (blue). Letters indicate significant differences between genotypes according to one-way ANOVA with *post hoc* LSD testing (*P* ≤ 0.05). nd, not determined.

levels (see also Fig. 3c), resulting in the negative correlation between sucrose levels and rosette branching. There was no significant correlation between Tre6P or the Tre6P : sucrose ratio based on whole rosette measurements. However, based on measurements of vascular enriched samples, both Tre6P and the Tre6P : sucrose ratio had a highly significant positive correlation with RI branch number per plant and an even stronger positive correlation with RI branch number per leaf (Fig. 6). Thus, theTre6P : sucrose ratio in the vasculature correlates best with the observed branching phenotypes in the *pGLDPA* lines.

Interaction between Tre6P and the BRC1 branching signal integrator

To investigate how Tre6P signalling in the vasculature might be integrated with other signalling pathways that regulate shoot branching, *pGLDPA:otsA* (line #1) was crossed with the *brc1-2* (*brc1*) and *flowering locus t-10* (*ft*) mutants. Homozygous F$_2$ plants were grown in a 16-h photoperiod, along with the parental lines, for determination of RI branch number.

The *pGLDPA:otsA* plants had more branches (on average 3.6 RI branches) than the wild-type Col-0 (on average 2.5 RI branches; Fig. 7a,c), confirming our previous results. The total number of RI branches was also increased in *brc1* (on average 9 RI branches) and increased still further in *brc1 × pGLDPA:otsA* plants (on average 15 RI branches; Fig. 7a,c). By contrast,

branching was almost abolished in both the *ft* and *ft × pGLDPA: otsA* plants (on average < 1 RI branch; Fig. 7b,c). As seen before, *pGLDPA:otsA* plants flowered earlier than wild-type plants, as did the *brc1 × pGLDPA:otsA* and *ft × pGLDPA:otsA* lines compared to their respective *brc1* and *ft* parents (Fig. S8). Given the differences in total leaf number, we also plotted RI branch number on a per rosette leaf basis. The *brc1 × pGLDPA:otsA* plants had the highest number of RI branches per leaf (1.0; Fig. 7c), indicating that every axillary rosette bud grew out in this line. The RI branch number per rosette leaf was lower in the *brc1* mutant (0.5), the *pGLDPA:otsA* line (0.3) and wild-type plants (0.15). The *ft* mutant (0.01) and the *ft-10 × pGLDPA:otsA* plants (0.02) had the lowest values. We confirmed these results in a second independent experiment with the same lines (Fig. S9).

In summary, the branching mutant analysis showed that loss of BRC1 and increased Tre6P in the vasculature had a strong additive effect on shoot branching, while increasing Tre6P in the vasculature in the *ft* mutant background had no impact on axillary bud outgrowth.

Discussion

Tre6P acts locally within axillary buds to modulate shoot branching

We previously demonstrated that the breaking of axillary bud dormancy in pea is associated with a rapid rise in bud Tre6P levels that is highly correlated with bud outgrowth (Fichtner *et al.*, 2017). In arabidopsis, we observed that the predominant Tre6P-synthesizing enzyme, TPS1, is expressed in axillary buds, and that complementation of the *tps1-1* mutant by expression of a heterologous TPS from *E. coli* (OtsA) restored shoot branching to wild-type levels (Fig. 1). Together, these results show that there is enzymatic capacity for Tre6P synthesis in axillary buds and that the influence of TPS1 on shoot branching is primarily due to its Tre6P-synthesizing activity rather than any non-catalytic (e.g. signalling) function. With TPS1 being present in the buds, we can infer that Tre6P is at least partly produced locally within the buds in response to any increase in their sucrose supply. Expressing CeTPP in buds to counteract any rise in their Tre6P levels led to delayed rosette branching in the *pBRC1: CeTPP* plants in long days (Fig. 2h) and the suppression of branching in short days (Fig. 2g), providing genetic evidence that Tre6P acts locally within axillary buds to modulate shoot branching.

We observed only relatively small metabolic changes when Tre6P levels were decreased specifically in axillary buds, via *pBRC1*-driven CeTPP expression. This might be simply a technical issue related to the tissue sampling. Although we sampled tissues (rosette cores) that should be enriched in cell types where the *BRC1* promoter is active, the harvested material still contained substantial amounts of tissue where the *BRC1* promoter is not active and changes in Tre6P in the targeted tissues could be partially or completely masked if metabolite levels were unaffected or changed in the opposite manner in other cell types. However, both *pBRC1:CeTPP* lines showed significantly lower
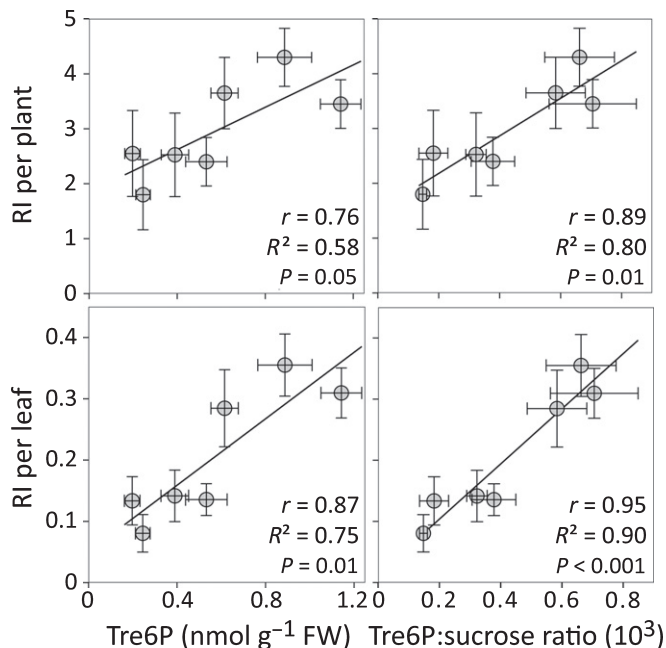
Fig. 6 Correlation analyses in arabidopsis plants with alteredtrehalose 6-phosphate (Tre6P) levels in the vasculature. The number of primary rosette (RI) branches per plant and per leaf of *pGLDPA:otsA*, *pGLDPA:CeTPP*, *pGLDPA:GUS*, *p35S:otsA* and wild-type Col-0 plants were plotted against the level of Tre6P and the Tre6P : sucrose ratio measured in vasculature-enriched tissue samples. Plants were grown in 16-h photoperiods. The Pearson correlation coefficient (*r*), coefficient of determination (*R*²) and probability (*P*) values for each relationship are indicated. Error bars indicate 95% confidence intervals.
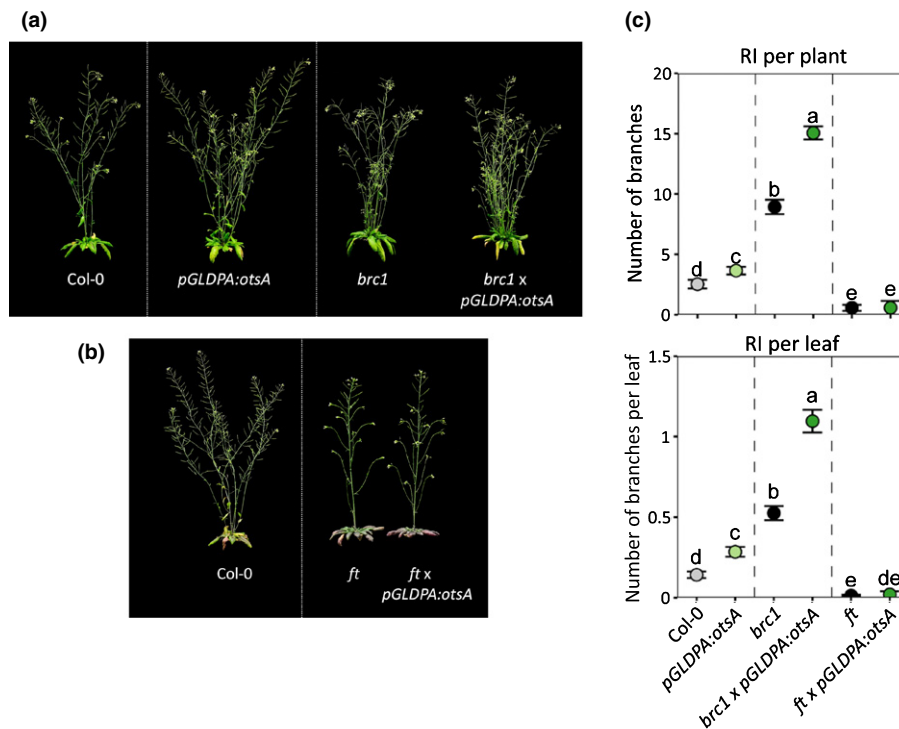
Fig. 7 Effects of vasculature-specific TPS overexpression in wild-type and branching mutant backgrounds on flowering and shoot branching under long-day conditions. Visual phenotypes of (a) *branched1* (*brc1*) and (b) *flowering locus t* (*ft*) mutants and plants expressing the *Escherichia coli* TPS (OtsA) in the vasculature (*pGLDPA:otsA*) in these mutant backgrounds grown in a 16-h photoperiod. Plants were grown in a 16-h photoperiod and photographed at 45 (a) or 56 (b) d after sowing (DAS). (c) Primary rosette (RI) branches per plant, flowering time based on total leaf number and RI branches per rosette leaf. Symbol colours: wild-type Col-0 (grey); *brc1*, *ft* parental mutants (black); *pGLDPA:otsA* expression in a wild-type background (light green); *pGLDPA:otsA* expression in a mutant background (dark green). The *pGLDPA:otsA* construct was introgressed into the *brc1* and *ft* mutant backgrounds by crossing the mutants with *pGLDPA:otsA* line #1. RI branches (length ≥ 0.5 cm) were counted at the end of the plant's life cycle. Data are presented as mean ± SEM (*n* = 11–19) and letters indicate significant differences between genotypes according to one-way ANOVA with *post hoc* LSD testing (*P* ≤ 0.05).

Tre6P : sucrose ratio at 21 DAS when axillary meristem development is active. Consistently, branch initiation was severely delayed when the Tre6P : sucrose ratio was decreased in axillary buds (*pBRC1:CeTPP* plants) under long-day conditions (Fig. 2h) and branching was inhibited short-days (i.e. C limiting conditions, Fig. 2g). Together with the demonstrated expression of TPS1 in axillary buds, these results provide genetic evidence that Tre6P acts locally within axillary buds to modulate branch initiation.

Tre6P levels in the vasculature regulate shoot branching in arabidopsis

The expression pattern of the *F. trinervia GLDPA* promoter is very similar to the expression domain of the *TPS1* gene in the vasculature (Fichtner *et al.*, 2020), providing a means to investigate the specific functions of Tre6P in the vasculature. The *pGLDPA:otsA* lines, with increased Tre6P levels only in the vasculature, displayed an increased branching phenotype to the same degree as *p35S:otsA* plants. Our observation that the *pGLDPA: CeTPP* plants had the opposite phenotype provides compelling evidence that these phenotypic differences were driven by changes in Tre6P. Furthermore, there was a strong correlation between shoot branching and the levels of Tre6P and Tre6P : sucrose ratio

in the vasculature. Given that TPS1 is expressed predominantly in the vasculature (Fichtner *et al.*, 2020) and the *pGLDPA:otsA* plants flowered early and had as many branches as *p35S:otsA* plants, we conclude that the vasculature is a primary location for Tre6P synthesis and signalling in the regulation of flowering and branching.

Potential mechanisms for regulation of shoot branching by Tre6P in the vasculature and in axillary buds

Altering Tre6P levels in the vasculature could affect shoot branching in several ways. Tre6P produced in the companion cell-sieve element complex of the vasculature is likely to move with the mass flow of solutes in the phloem and be delivered to distal sink organs, such as axillary buds, where it might supplement Tre6P made locally by the TPS1 enzyme in the buds (Fig. 8). In principle, grafting experiments with *tps1* null mutants would be the simplest approach for testing whether Tre6P does move from source to sink organs via the phloem, but such experiments are not feasible due to the defective embryogenesis in *tps1* null mutants that makes these mutants nonviable (Eastmond *et al.*, 2002).

Tre6P could also have indirect effects in the vasculature by influencing sucrose allocation (Fig. 8). For example, the observed
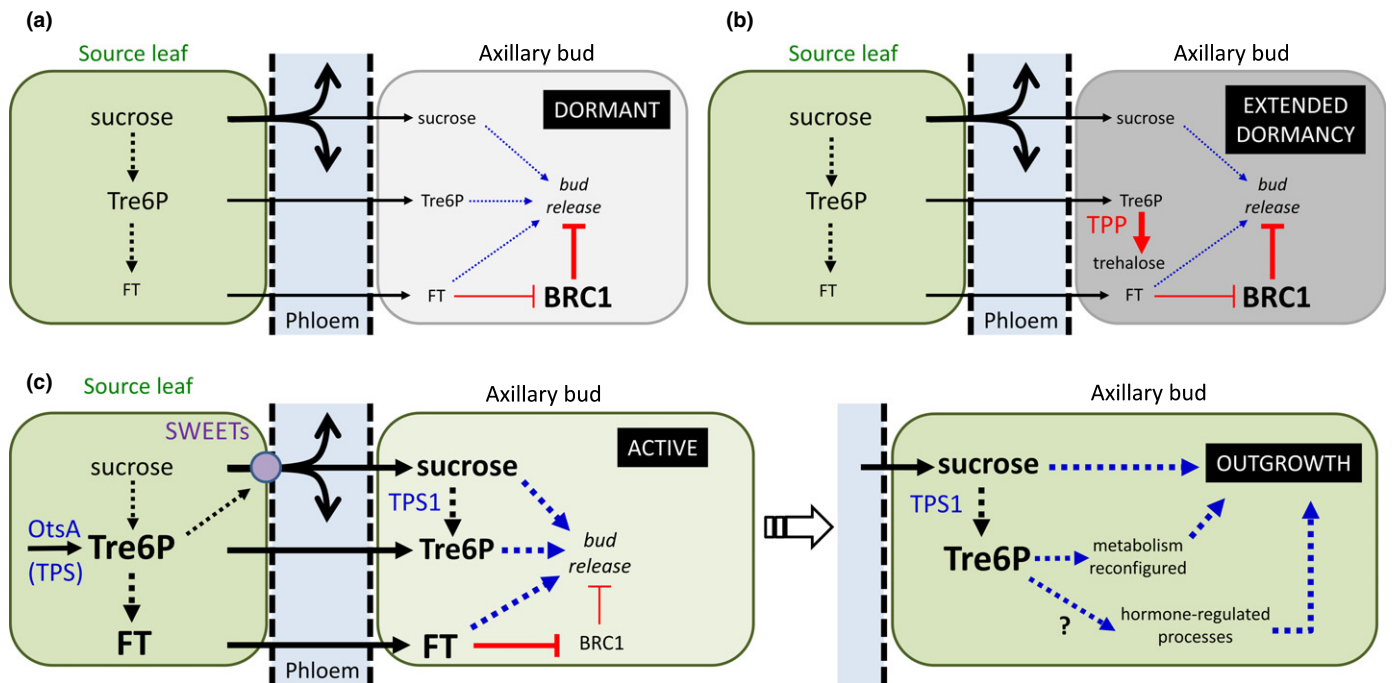
Fig. 8 Schematic model for the role of trehalose 6-phosphate (Tre6P) in axillary bud outgrowth in arabidopsis. (a) Limited supply of sucrose to axillary buds and strong expression of BRANCHED1 (BRC1) maintains bud dormancy. (b) Bud-specific expression of a heterologous TPP in *pBRC1:CeTPP* lines lowers Tre6P levels in the buds, further delaying their release from dormancy. (c) Expression of a heterologous TPS (OtsA) in *pGLDPA:otsA* lines increases Tre6P in the phloem parenchyma and companion cell-sieve element complex in leaf veins, leading to upregulation of SWEET sucrose efflux carries, enhanced phloem loading of sucrose and increased sucrose supply to axillary buds. Higher sucrose levels stimulate local synthesis of Tre6P in the buds by TPS1 (additional Tre6P might also move from leaves to buds via the phloem). In parallel, high Tre6P in companion cells stimulates expression of *FLOWERING LOCUS T* (*FT*). Movement of the phloem-mobile FT protein to buds leads to inhibition of BRC1. High sucrose, high Tre6P and FT act synergistically in the buds to trigger the release of dormancy. Following release from dormancy, Tre6P sustains bud outgrowth by coordinating a reconfiguration of bud metabolism for growth, and via interaction with hormone-regulated processes (e.g. stimulating establishment of polar auxin transport from the new shoot). Solid black arrows represent metabolic fluxes or transport steps. Dashed blue arrows and red lines represent positive and negative regulatory processes, respectively, with line width representing the strength of the response.

upregulation of *SWEET11*, *SWEET12* and *SWEET13* in source leaves in *pGLDPA:otsA* plants (Figs 3f, 4a) and downregulation of *SUC2*, *SWEET11*, *SWEET12* and *SWEET13* in *pGLDPA: CeTPP* plants (Fig. S4) could increase or decrease, respectively, the export of sucrose from source leaves and this the potential supply of sucrose to sink organs, including axillary buds. SWEET-type sucrose efflux carriers are also involved in phloem unloading in many sink organs (Eom *et al.*, 2015; Milne *et al.*, 2017) and *SWEET13* and *SWEET14* are expressed in or nearby axillary buds (Kanno *et al.*, 2016). Therefore, the observed upregulation of *SWEET13* and *SWEET14* in rosette cores of the *pGLDPA:otsA* plants could indicate increased capacity to deliver sucrose to axillary buds and the SAM. Increasing the supply of sucrose to axillary buds via such mechanisms would not only provide more carbon and energy for growth, but could also trigger their release from dormancy and growth into new shoots through a signalling pathway (Mason *et al.*, 2014). In accordance, lowering Tre6P in developing maize seeds led to increased yield under well-watered or drought conditions that correlated with upregulation of *SWEET* transporter genes (Nuccio *et al*, 2015; Oszvald *et al.*, 2018). Overexpression of SWEETs also leads to more axillary growth in *Chrysanthemum morifolium* (Liu *et al.*, 2020) and early flowering in arabidopsis (Andrés *et al.*, 2020).

A third possibility is that altered Tre6P levels in the vasculature affect other systemic signalling components and pathways that influence shoot branching. In arabidopsis, the expression of *FT* is triggered by long days, under the control of CO, and is dependent on the Tre6P-synthesizing activity of TPS1 (Wahl *et al.*, 2013; Fichtner *et al.*, 2020). FT can also move via the phloem to axillary meristems, and promote their elongation and development by activating their floral transition (Niwa *et al.*, 2013; Tsuji *et al.*, 2015). Plants with higher Tre6P in the vasculature have early flowering and increased branching phenotypes, and we observed significant increases in *CO*, *FT* and *TSF* transcript abundance in the *pGLDPA:otsA* plants (Fig. 4b). This suggested that increased Tre6P levels in the vasculature induced *CO* expression, thereby increasing expression of *FT* and *TSF*, which in turn could result in early flowering and increased branching (Fig. 8). Accordingly, stimulation of branching by increased Tre6P in the vasculature was abolished in an *ft* mutant background (Fig. 7b,c), suggesting that FT is a crucial factor in the ability of axillary buds to respond to distal changes in Tre6P levels (Fig. 8).

We also showed that increasing Tre6P in a *brc1* mutant background has a strong additive effect on branching. This suggests that the stimulation of FT expression in the leaf vasculature and loss of the FT repressor in axillary buds (i.e. BRC1) act synergistically to bring about the strong branching phenotype of the

brc1 × *pGLDPA:otsA* plants. In arabidopsis and wheat, the FT protein (also TSF in arabidopsis) has been shown to interact directly with BRC1, and this interaction leads to a reciprocal repressive effect, i.e. FT and BRC1 inhibit each other (Niwa *et al.*, 2013; Dixon *et al.*, 2018). Enhanced *FT* expression in the *pGLDPA:otsA* lines could lead to an accumulation of FT protein in the buds shifting the FT : BRC1 ratio in favour of FT leading to the stimulation of bud outgrowth (Fig. 8). It was recently reported that a potato (*Solanum tuberosum*) tuber-specific isoform of FT (StSP6A) can interact with StSWEET11 to block the leakage of sucrose to the apoplast and promote symplastic transport of sucrose (Abelenda *et al.*, 2019). Such switches in the pathway of sucrose delivery are a common feature during the development and growth of sink organs (Weber *et al.*, 1988; Eom *et al.*, 2015; Milne *et al.*, 2017). Thus, distal changes in Tre6P could affect the delivery of sucrose to axillary buds via changes in *SWEET* expression, or as described earlier, via FT-mediated changes in the pathway of phloem unloading in the buds, or both.

Lowering bud Tre6P levels, by *pBRC1*-driven expression of CeTPP, delayed bud outgrowth in long days and suppressed branching in short days, providing genetic evidence that Tre6P acts locally within axillary buds to modulate shoot branching. This suggests that Tre6P, either by itself or by potentiating the effect of other signals (e.g. phytohormones), is involved in modulating bud outgrowth. Low bud Tre6P levels could also compromise Tre6P-driven changes in central metabolism that are needed for sustained outgrowth (Fichtner *et al.*, 2017). In addition, there are several lines of evidence that Tre6P associated changes in bud metabolism might also have an impact on auxin synthesis and signalling. Tre6P promotes the expression of the auxin biosynthesis gene *TRYPTOPHAN AMINOTRANSFERASE RELATED2* in pea seeds (Meitzel *et al.*, 2021) and PINOID1 (PIN1) auxin efflux proteins become delocalized in meristems when plants have low C status (Lauxmann *et al.*, 2016) and therefore low Tre6P levels (Lunn *et al.*, 2006).

IIn conclusion, we provide genetic evidence that Tre6P acts locally in axillary buds, showing that Tre6P in buds is not only correlated with growth (Fichtner *et al.*, 2017), but also necessary for bud outgrowth. Our results also implicate Tre6P in systemic regulation of bud outgrowth, acting in the vasculature to signal the overall sucrose status of the plant and control sucrose allocation, and being linked to photoperiod signalling by FT under long-day conditions. We postulate that Tre6P is a key factor linking shoot branching to carbon availability, enabling plants to sense and allocate their carbon resources to an appropriate number of shoot branches, thus helping to optimize shoot architecture for survival and reproductive success. In future experiments, the level of Tre6P in the vasculature and axillary buds could be a target for engineering improvements in crop architecture.

Author contributions

CAB, MS and JEL conceived the project. FF designed and performed all experiments and measurements with help from FFB and MGA. RF performed Tre6P measurements. JJO and BM-R performed sectioning and helped with imaging of stained sections. FF and JEL wrote the manuscript with help from FFB, MS and CAB. All authors commented on the manuscript and approved the final version.

ORCID

Maria G. Annunziata (iD) https://orcid.org/0000-0001-8593-1741
Francois F. Barbier (iD) https://orcid.org/0000-0002-1177-1930
Christine A. Beveridge (iD) https://orcid.org/0000-0003-0878-3110
Regina Feil (iD) https://orcid.org/0000-0002-9936-1337
Franziska Fichtner (iD) https://orcid.org/0000-0002-4508-5437
John E. Lunn (iD) https://orcid.org/0000-0001-8533-3004
Bernd Mueller-Roeber (iD) https://orcid.org/0000-0002-1410-464X
Justyna J. Olas (iD) https://orcid.org/0000-0002-4311-6738
Mark Stitt (iD) https://orcid.org/0000-0002-4900-1763

References

Abelenda JA, Bergonzi S, Oortwijn M, Sonnewald S, Du M, Visser RG, Sonnewald U, Bachem CWB. 2019. Source–sink regulation is mediated by interaction of an FT homolog with a SWEET protein in potato. *Current Biology* 29: 1178–1186.e6.

Aguilar-Martinez JA, Poza-Carrion C, Cubas P. 2007. Arabidopsis BRANCHED1 acts as an integrator of branching signals within axillary buds. *Plant Cell* 19: 458–472.

Andrés F, Kinoshita A, Kalluri N, Fernández V, Falavigna VS, Cruz TMD, Jang S, Chiba Y, Seo M, Mettler-Altmann T *et al.* 2020. The sugar transporter SWEET10 acts downstream of *FLOWERING LOCUS T* during floral transition of *Arabidopsis thaliana*. *BMC Plant Biology* 20: 1–14.

Annunziata MG, Apelt F, Carillo P, Krause U, Feil R, Mengin V, Lauxmann MA, Köhl K, Nikoloski Z, Stitt M *et al.* 2017. Getting back to nature: a reality check for experiments in controlled environments. *Journal of Experimental Botany* 68: 4463–4477.

Aubry S, Smith-Unna RD, Boursnell CM, Kopriva S, Hibberd JM. 2014. Transcript residency on ribosomes reveals a key role for the *Arabidopsis thaliana* bundle sheath in sulfur and glucosinolate metabolism. *The Plant Journal* 78: 659–673.

Baker RF, Leach KA, Braun DM. 2012. SWEET as sugar: new sucrose effluxers in plants. *Molecular Plant* 5: 766–768.

Barbier FF, Chabikwa TG, Ahsan MU, Cook SE, Powell R, Tanurdzic M, Beveridge CA. 2019a. A phenol/chloroform-free method to extract nucleic acids from recalcitrant, woody tropical species for gene expression and sequencing. *Plant Methods* 15: 62.

Barbier FF, Dun EA, Kerr SC, Chabikwa TG, Beveridge CA. 2019b. An update on the signals controlling shoot branching. *Trends in Plant Science* 24: 220–236.

Barbier FF, Lunn JE, Beveridge CA. 2015a. Ready, steady, go! A sugar hit starts the race to shoot branching. *Current Opinion in Plant Biology* 25: 39–45.

Barbier FF, Peron T, Lecerf M, Perez-Garcia MD, Barriere Q, Rolcik J, Boutet-Mercey S, Citerne S, Lemoine R, Porcheron B et al. 2015b. Sucrose is an early modulator of the key hormonal mechanisms controlling bud outgrowth in *Rosa hybrida*. *Journal of Experimental Botany* 66: 2569–2582.

Bertheloot J, Barbier F, Boudon F, Perez-Garcia MD, Péron T, Citerne S, Dun E, Beveridge C, Godin C, Sakr S. 2020. Sugar availability suppresses the auxin-induced strigolactone pathway to promote bud outgrowth. *New Phytologist* 225: 866–879.

Beveridge CA, Murfet IC. 1996. The *gigas* mutant in pea is deficient in the floral stimulus. *Physiologia Plantarum* 96: 637–645.

Bledsoe SW, Henry C, Griffiths CA, Paul MJ, Feil R, Lunn JE, Stitt M, Lagrimini LM. 2017. The role of Tre6P and SnRK1 in maize early kernel development and events leading to stress-induced kernel abortion. *BMC Plant Biology* 17: 74.

Braun N, de Saint Germain A, Pillot JP, Boutet-Mercey S, Dalmais M, Antoniadi I, Li X, Maia-Grondard A, Le Signor C, Bouteiller N et al. 2012. The pea TCP transcription factor PsBRC1 acts downstream of strigolactones to control shoot branching. *Plant Physiology* 158: 225–238.

Brewer PB, Dun EA, Ferguson BJ, Rameau C, Beveridge CA. 2009. Strigolactone acts downstream of auxin to regulate bud outgrowth in pea and arabidopsis. *Plant Physiology* 150: 482–493.

Brewer PB, Koltai H, Beveridge CA. 2013. Diverse roles of strigolactones in plant development. *Molecular Plant* 6: 18–28.

Chen LQ, Qu XQ, Hou BH, Sosso D, Osorio S, Fernie AR, Frommer WB. 2012. Sucrose efflux mediated by SWEET proteins as a key step for phloem transport. *Science* 335: 207–211.

Claeys H, Vi S, Xu X, Satoh-Nagasawa N, Eveland A, Goldshmidt A, Feil R, Beggs G, Sakai H, Brennan R et al. 2019. Control of meristem determinacy by trehalose-6-phosphate phosphatases is uncoupled from enzymatic activity. *Nature Plants* 5: 352.

Clough SJ, Bent AF. 1998. Floral dip: a simplified method for agrobacterium-mediated transformation of *Arabidopsis thaliana*. *The Plant Journal* 16: 735–743.

Delorge I, Figueroa CM, Feil R, Lunn JE, Van Dijck P. 2015. TREHALOSE-6-PHOSPHATE SYNTHASE 1 is not the only active TPS in *Arabidopsis thaliana*. *Biochemical Journal* 466: 283–290.

Dixon LE, Greenwood JR, Bencivenga S, Zhang P, Cockram J, Mellers G, Ramm K, Cavanagh C, Swain SM, Boden SA. 2018. TEOSINTE BRANCHED1 regulates inflorescence architecture and development in bread wheat (*Triticum aestivum* L.). *Plant Cell* 30: 563–581.

Domagalska MA, Leyser O. 2011. Signal integration in the control of shoot branching. *Nature Review Molecular Cell Biology* 12: 211–221.

Dong Z, Xiao Y, Govindarajulu R, Feil R, Siddoway ML, Nielsen T, Lunn JE, Hawkins J, Chuck G. 2019. The regulatory landscape of a core maize domestication module controlling bud dormancy and growth repression. *Nature Communications* 10: 1–15.

Dun EA, Brewer PB, Beveridge CA. 2009. Strigolactones: discovery of the elusive shoot branching hormone. *Trends in Plant Sciences* 14: 364–372.

Dun EA, de Saint Germain A, Rameau C, Beveridge CA. 2012. Antagonistic action of strigolactone and cytokinin in bud outgrowth control. *Plant Physiology* 158: 487–498.

Dun EA, de Saint Germain A, Rameau C, Beveridge CA. 2013. Dynamics of strigolactone function and shoot branching responses in *Pisum sativum*. *Molecular Plant* 6: 128–140.

Eastmond PJ, van Dijken AJH, Spielman M, Kerr A, Tissier AF, Dickinson HG, Jones JDG, Smeekens SC, Graham IA. 2002. Trehalose-6-phosphate synthase 1, which catalyses the first step in trehalose synthesis, is essential for arabidopsis embryo maturation. *The Plant Journal* 29: 225–235.

Engelmann S, Wiludda C, Burscheidt J, Gowik U, Schlue U, Koczor M, Streubel M, Cossu R, Bauwe H, Westhoff P. 2008. The gene for the P-subunit of glycine decarboxylase from the C_4 species *Flaveria trinervia*: analysis of transcriptional control in transgenic *Flaveria bidentis* (C_4) and arabidopsis (C_3). *Plant Physiology* 146: 1773–1785.

Eom JS, Chen LQ, Sosso D, Julius BT, Lin IW, Qu XQ, Braun DM, Frommer WB. 2015. SWEETs, transporters for intracellular and intercellular sugar translocation. *Current Opinion in Plant Biology* 25: 53–62.

Ferguson BJ, Beveridge CA. 2009. Roles for auxin, cytokinin, and strigolactone in regulating shoot branching. *Plant Physiology* 149: 1929–1944.

Fichtner F, Barbier FF, Feil R, Watanabe M, Annunziata MG, Chabikwa TG, Höfgen R, Stitt M, Beveridge CA, Lunn JE. 2017. Trehalose 6-phosphate is involved in triggering axillary bud outgrowth in garden pea (*Pisum sativum* L.). *The Plant Journal* 92: 611–623.

Fichtner F, Lunn JE. In press. The role of trehalose 6-phosphate (Tre6P) in plant metabolism and development. *Annual Review of Plant Biology* 72: doi: 10.1146/annurev-arplant-050718-095929.

Fichtner F, Olas JJ, Feil R, Watanabe M, Krause U, Hoefgen R, Stitt M, Lunn JE. 2020. Functional features of TREHALOSE-6-PHOSPHATE SYNTHASE1 – an essential enzyme in *Arabidopsis thaliana*. *Plant Cell* 32: 1949–1972.

Figueroa CM, Feil R, Ishihara H, Watanabe M, Kolling K, Krause U, Hohne M, Encke B, Plaxton WC, Zeeman SC et al. 2016. Trehalose 6-phosphate coordinates organic and amino acid metabolism with carbon availability. *The Plant Journal* 85: 410–423.

Figueroa CM, Lunn JE. 2016. A tale of two sugars: trehalose 6-phosphate and sucrose. *Plant Physiology* 172: 7–27.

Flis A, Fernández AP, Zielinski T, Mengin V, Sulpice R, Stratford K, Hume A, Pokhilko A, Southern MM, Seaton DD et al. 2015. Defining the robust behaviour of the plant clock gene circuit with absolute RNA timeseries and open infrastructure. *Open Biology* 5: 150042.

Gomez-Roldan V, Fermas S, Brewer PB, Puech-Pages V, Dun EA, Pillot JP, Letisse F, Matusova R, Danoun S, Portais JC et al. 2008. Strigolactone inhibition of shoot branching. *Nature* 455: 189–194.

Hecht V, Laurie RE, Vander Schoor JK, Ridge S, Knowles CL, Liew LC, Sussmilch FC, Murfet IC, Macknight RC, Weller JL. 2011. The pea *GIGAS* gene is a *FLOWERING LOCUS T* homolog necessary for graft-transmissible specification of flowering but not for responsiveness to photoperiod. *Plant Cell* 23: 147–161.

Hellens RP, Edwards EA, Leyland NR, Bean S, Mullineaux PM. 2000. pGreen: a versatile and flexible binary Ti vector for agrobacterium-mediated plant transformation. *Plant Molecular Biology* 42: 819–832.

Kanno Y, Oikawa T, Chiba Y, Ishimaru Y, Shimizu T, Sano N, Koshiba T, Kamiya Y, Ueda M, Seo M. 2016. AtSWEET13 and AtSWEET14 regulate gibberellin-mediated physiological processes. *Nature Communications* 7: 1–11.

Kebrom TH, Brutnell TP, Finlayson SA. 2010. Suppression of sorghum axillary bud outgrowth by shade, phyB and defoliation signalling pathways. *Plant, Cell and Environment* 33: 48–58.

Kebrom TH, Chandler PM, Swain SM, King RW, Richards RA, Spielmeyer W. 2012. Inhibition of tiller bud outgrowth in the *tin* mutant of wheat is associated with precocious internode development. *Plant Physiology* 160: 308–318.

Kebrom TH, Mullet JE. 2016. Transcriptome profiling of tiller buds provides new insights into PhyB regulation of tillering and indeterminate growth in sorghum. *Plant Physiology* 170: 2232–2250.

Kormish JD, McGhee JD. 2005. The *C. elegans* lethal *gut-obstructed gob-1* gene is trehalose-6-phosphate phosphatase. *Developmental Biology* 287: 35–47.

Lalonde S, Tegeder M, Throne-Holst M, Frommer W, Patrick J. 2003. Phloem loading and unloading of sugars and amino acids. *Plant, Cell & Environment* 26: 37–56.

Lauxmann MA, Annunziata MG, Brunoud G, Wahl V, Koczut A, Burgos A, Olas JJ, Maximova E, Abel C, Schlereth A et al. 2016. Reproductive failure in *Arabidopsis thaliana* under transient carbohydrate limitation: flowers and very young siliques are jettisoned and the meristem is maintained to allow successful resumption of reproductive growth. *Plant, Cell & Environment* 39: 745–767.

Li C, Zhang Y, Zhang K, Guo D, Cui B, Wang X, Huang X. 2015. Promoting flowering, lateral shoot outgrowth, leaf development, and flower abscission in tobacco plants overexpressing cotton *FLOWERING LOCUS T* (*FT*)-like gene *GhFT1*. *Frontiers in Plant Science* **6**: 454.

Liu W, Peng B, Song A, Jiang J, Chen F. 2020. Sugar transporter, CmSWEET17, promotes bud outgrowth in *Chrysanthemum morifolium*. *Genes* **11**: 26.

Lunn JE, Feil R, Hendriks JH, Gibon Y, Morcuende R, Osuna D, Scheible WR, Carillo P, Hajirezaei MR, Stitt M. 2006. Sugar-induced increases in trehalose 6-phosphate are correlated with redox activation of ADP glucose pyrophosphorylase and higher rates of starch synthesis in *Arabidopsis thaliana*. *Biochemical Journal* **397**: 139–148.

Martín-Fontecha ES, Tarancón C, Cubas P. 2018. To grow or not to grow, a power-saving program induced in dormant buds. *Current Opinion in Plant Biology* **41**: 102–109.

Martins MC, Hejazi M, Fettke J, Steup M, Feil R, Krause U, Arrivault S, Vosloh D, Figueroa CM, Ivakov A et al. 2013. Feedback inhibition of starch degradation in arabidopsis leaves mediated by trehalose 6-phosphate. *Plant Physiology* **163**: 1142–1163.

Mason MG, Ross JJ, Babst BA, Wienclaw BN, Beveridge CA. 2014. Sugar demand, not auxin, is the initial regulator of apical dominance. *Proceedings of the National Academy of Sciences, USA* **111**: 6092–6097.

Meitzel T, Radchuk R, McAdam EL, Thormählen I, Feil R, Munz E, Hilo A, Geigenberger P, Ross JJ, Lunn JE et al. 2021. Trehalose 6-phosphate promotes seed filling by activating auxin biosynthesis. *New Phytologist* **229**: 1553–1565.

Milne RJ, Perroux JM, Rae AL, Reinders A, Ward JM, Offler CE, Patrick JW, Grof CPL. 2017. Sucrose transporter localization and function in phloem unloading in developing stems. *Plant Physiology* **173**: 1330–1341.

Muller D, Leyser O. 2011. Auxin, cytokinin and the control of shoot branching. *Annals of Botany* **107**: 1203–1212.

Murashige T, Skoog F. 1962. A revised medium for rapid growth and bio assays with tobacco tissue cultures. *Physiologia Plantarum* **15**: 473–497.

Niwa M, Daimon Y, Kurotani K, Higo A, Pruneda-Paz JL, Breton G, Mitsuda N, Kay SA, Ohme-Takagi M, Endo M et al. 2013. BRANCHED1 interacts with FLOWERING LOCUS T to repress the floral transition of the axillary meristems in arabidopsis. *Plant Cell* **25**: 1228–1242.

Nuccio ML, Wu J, Mowers R, Zhou H-P, Meghji M, Primavesi LF, Paul MJ, Chen X, Gao Y, Haque E et al. 2015. Expression of trehalose-6-phosphate phosphatase in maize ears improves yield in well-watered and drought conditions. *Nature Biotechnology* **33**: 862–869.

Nunes C, O'Hara LE, Primavesi LF, Delatte TL, Schluepmann H, Somsen GW, Silva AB, Fevereiro PS, Wingler A, Paul MJ. 2013. The trehalose 6-phosphate/SnRK1 signaling pathway primes growth recovery following relief of sink limitation. *Plant Physiology* **162**: 1720–1732.

Olas JJ, Van Dingenen J, Abel C, Działo MA, Feil R, Krapp A, Schlereth A, Wahl V. 2019. Nitrate acts at the *Arabidopsis thaliana* shoot apical meristem to regulate flowering time. *New Phytologist* **223**: 814–827.

Osuna D, Usadel B, Morcuende R, Gibon Y, Blasing OE, Hohne M, Günter M, Kamlage B, Trethewey R, Scheible WR et al. 2007. Temporal responses of transcripts, enzyme activities and metabolites after adding sucrose to carbon-deprived arabidopsis seedlings. *The Plant Journal* **49**: 463–491.

Oszvald M, Primavesi LF, Griffiths CA, Cohn J, Basu S, Nuccio ML, Paul MJ. 2018. Trehalose 6-phosphate regulates photosynthesis and assimilate partitioning in reproductive tissue. *Plant Physiology* **176**: 2623–2638.

Patrick JW, Colyvas K. 2014. Crop yield components – photoassimilate supply- or utilisation limited-organ development? *Functional Plant Biology* **41**: 893–913.

Prusinkiewicz P, Crawford S, Smith RS, Ljung K, Bennett T, Ongaro V, Leyser O. 2009. Control of bud activation by an auxin transport switch. *Proceedings of the National Academy of Sciences, USA* **106**: 17431–17436.

Radchuk R, Emery RJN, Weier D, Vigeolas H, Geigenberger P, Lunn JE, Feil R, Weschke W, Weber H. 2010. Sucrose non-fermenting 1 (SnRK1) coordinates metabolic and hormonal signals during pea cotyledon growth and differentiation. *The Plant Journal* **61**: 324–338.

Ramon M, De Smet I, Vandesteene L, Naudts M, Leyman B, Van Dijck P, Rolland F, Beeckman T, Thevelein JM. 2009. Extensive expression regulation

and lack of heterologous enzymatic activity of the Class II trehalose metabolism proteins from *Arabidopsis thaliana*. *Plant, Cell & Environment* **32**: 1015–1032.

Sachs T, Thimann KV. 1967. The role of auxins and cytokinins in the release of buds from dominance. *American Journal of Botany* **54**: 136–144.

Satoh-Nagasawa N, Nagasawa N, Malcomber S, Sakai H, Jackson D. 2006. A trehalose metabolic enzyme controls inflorescence architecture in maize. *Nature* **441**: 227–230.

Schluepmann H, Pellny T, van Dijken A, Smeekens S, Paul M. 2003. Trehalose 6-phosphate is indispensable for carbohydrate utilization and growth in *Arabidopsis thaliana*. *Proceedings of the National Academy of Sciences, USA* **100**: 6849–6854.

Shimizu-Sato S, Tanaka M, Mori H. 2009. Auxin-cytokinin interactions in the control of shoot branching. *Plant Molecular Biology* **69**: 429–435.

Stitt M, Lilley RM, Gerhardt R, Heldt HW. 1989. Metabolite levels in specific cells and subcellular compartments of plant leaves. *Methods in Enzymology* **174**: 518–552.

Tarancón C, González-Grandío E, Oliveros JC, Nicolas M, Cubas P. 2017. A conserved carbon starvation response underlies bud dormancy in woody and herbaceous species. *Frontiers in Plant Science* **8**: 788.

Tsuji H, Tachibana C, Tamaki S, Taoka K, Kyozuka J, Shimamoto K. 2015. Hd3a promotes lateral branching in rice. *The Plant Journal* **82**: 256–266.

Turck F, Fornara F, Coupland G. 2008. Regulation and identity of florigen: FLOWERING LOCUS T moves center stage. *Annual Review of Plant Biology* **59**: 573–594.

Umehara M, Hanada A, Yoshida S, Akiyama K, Arite T, Takeda-Kamiya N, Magome H, Kamiya Y, Shirasu K, Yoneyama K et al. 2008. Inhibition of shoot branching by new terpenoid plant hormones. *Nature* **455**: 195–200.

Wahl V, Ponnu J, Schlereth A, Arrivault S, Langenecker T, Franke A, Feil R, Lunn JE, Stitt M, Schmid M. 2013. Regulation of flowering by trehalose-6-phosphate signaling in *Arabidopsis thaliana*. *Science* **339**: 704–707.

Weber H, Heim U, Golombek S, Borisjuk L, Manteuffel R, Wobus U. 1998. Expression of a yeast-derived invertase in developing cotyledons of *Vicia narbonensis* alters the carbohydrate state and affects storage functions. *The Plant Journal* **16**: 163–172.

Weng L, Bai X, Zhao F, Li R, Xiao H. 2016. Manipulation of flowering time and branching by overexpression of the tomato transcription factor SlZFP2. *Plant Biotechnology Journal* **14**: 2310–2321.

Wickson M, Thimann KV. 1958. The antagonism of auxin and kinetin in apical dominance. *Physiologia Plantarum* **11**: 62–74.

Wiludda C, Schulze S, Gowik U, Engelmann S, Koczor M, Streubel M, Bauwe H, Westhoff P. 2012. Regulation of the photorespiratory *GLDPA* gene in C₄ *Flaveria*: an intricate interplay of transcriptional and posttranscriptional processes. *Plant Cell* **24**: 137–151.

Yadav UP, Ivakov A, Feil R, Duan GY, Walther D, Giavalisco P, Piques M, Carillo P, Hubberten HM, Stitt M et al. 2014. The sucrose-trehalose 6-phosphate (Tre6P) nexus: specificity and mechanisms of sucrose signalling by Tre6P. *Journal of Experimental Botany* **65**: 1051–1068.

Zakhartsev M, Medvedeva I, Orlov Y, Akberdin I, Krebs O, Schulze WX. 2016. Metabolic model of central carbon and energy metabolisms of growing *Arabidopsis thaliana* in relation to sucrose translocation. *BMC Plant Biology* **16**: 262.

Supporting Information

Additional Supporting Information may be found online in the Supporting Information section at the end of the article.

Fig. S1 Tissue specific expression patterns of the *GLDPA* and the *BRC1* promoters in arabidopsis.

Fig. S2 Rosette morphology of arabidopsis plants expressing a heterologous TPP under the control of an axillary bud-specific promoter (long-day conditions).

Fig. S3 Flowering time of TPS and TPP overexpression lines.

Fig. S4 Gene expression analyses in arabidopsis plants with constitutive or vascular-specific alterations in Tre6P.

Fig. S5 Rosette morphology of arabidopsis plants expressing heterologous TPS or TPP under the control of constitutive or vasculature-specific promoters (long-day conditions).

Fig. S6 Cauline branching phenotype of arabidopsis plants expressing a heterologous TPS under the control of constitutive or vasculature-specific promoters.

Fig. S7 Branching phenotype of the vascular-specific TPS and TPP overexpression lines after a shift from short-day to long-day conditions.

Fig. S8 Effects of vasculature-specific TPS overexpression in wild-type and branching mutant backgrounds on flowering time under long-day conditions.

Fig. S9 Effects of vasculature-specific TPS overexpression in wild-type and branching mutant backgrounds on flowering and shoot branching under long-day conditions (independent experiment).

Table S1 Oligonucleotide primers used for qRT-PCR analysis.

Please note: Wiley Blackwell are not responsible for the content or functionality of any Supporting Information supplied by the authors. Any queries (other than missing material) should be directed to the *New Phytologist* Central Office.

About *New Phytologist*

- *New Phytologist* is an electronic (online-only) journal owned by the New Phytologist Foundation, a **not-for-profit organization** dedicated to the promotion of plant science, facilitating projects from symposia to free access for our Tansley reviews and Tansley insights.

- Regular papers, Letters, Research reviews, Rapid reports and both Modelling/Theory and Methods papers are encouraged. We are committed to rapid processing, from online submission through to publication 'as ready' via *Early View* – our average time to decision is <26 days. There are **no page or colour charges** and a PDF version will be provided for each article.

- The journal is available online at Wiley Online Library. Visit **www.newphytologist.com** to search the articles and register for table of contents email alerts.

- If you have any questions, do get in touch with Central Office (np-centraloffice@lancaster.ac.uk) or, if it is more convenient, our USA Office (np-usaoffice@lancaster.ac.uk)

- For submission instructions, subscription and all the latest information visit **www.newphytologist.com**